DILLA UNIVERSITY

SCHOOL OF POSTGRADUATE STUDY

COLLAGE OF NATURAL AND COMPUTITIONAL SCIENCES

DEPARTEMENT OF PHYSICS

MSc THESIS ON:

COMMENSURATE MAGNETISM AND SUPERCONDUCTIVITY IN ELECTRON-DOPED BARIUM IRON ARSENIDE (Ba $(Fe_{1-x}Co_x)_2$ As_2) SUPERCONDUCTOR

BY: - FAYERA GASHU OLIKA

ADVISOR: - Dr. GIRMA KITACHEW

MSc THESIS SUBMITTED TO THE DEPARTMENT OF PHYSICS

FEBRUARY, 2023(G.C)

DILLA, ETHIOPIA

APPROVAL SHEET

DILLA UNIVERSITY

SCHOOL OF POSTGRADUATE STUDY

COLLAGE OF NATURAL AND COMPUTITIONAL SCIENCES

DEPARTEMENT OF PHYSICS

TITLE: *COMMENSURATE MAGNETISM AND SUPERCONDUCTIVITY IN ELECTRON DOPED BARIUM IRON ARSENIDE* ($Ba(Fe_{1-x}Co_x)_2As_2$) *SUPERCONDUCTOR*

THESIS SUBMITTED TO SCHOOL OF GRADUATE STUDIES FOR THE REQUIREMENT OF MASTERS DEGREE IN PHYSICS

--	-------------------	--------------------
NAME OF STUDENT	**SIGNATURE**	**DATE**
--	-------------------	--------------------
NAME OF ADVISOR	**SIGNATURE**	**DATE**
--	-------------------	--------------------
NAME OF EXTERNAL EXAMINER	**SIGNATURE**	**DATE**
--	-------------------	--------------------
NAME OF INTERNAL EXAMINER	**SIGNATURE**	**DATE**

ACKNOWLEDGMENTS

First of all, the work I report in this thesis would never have been possible without the support of GOD. I would like to say, thank you my God, for that you help me in everything.

Next I would like to express my deepest gratitude to my advisor Girma Kitachew (Ph.D.) for his assistance and encouragement to wards the completion of this proposal. I would like to extend my heartfelt thanks to everyone from whom I have learned so much over the past few years.

And also, I would like to appreciate my father Gashu Olika and my wife Dabale Kabade for their willingness in giving me moral, technical and materials support.

Finally, my thinks also goes to my mother Boje Hirpa, my daughter Yerosan Fayera, my son Jinenus Fayera, my eldest sister Chaltu Gashu, all my parents and my friends for their ideas and supports at any challenges and moments.

ABSTRACTS

A proper and accurate definition of the structural, magnetic, electronic phase boundaries and phase diagrams provides an extremely powerful tool to study commensurate magnetism and superconductivity in electron-doped barium iron arsenide superconductor. In this research work, the theoretical investigation of the coexistence of spin density wave and superconductivity in direct electron-doping at the Fe site with Co,($Ba(Fe_{1-x}Co_x)_2As_2$)has been made. We consider the interplay between superconducting (SC) and commensurate spin-density-wave (SDW) orders in iron-pnictides to answer, the questions such as what is the phase diagram of cobalt doped barium iron arsenide($Ba(Fe_{1-x}Co_x)_2As_2$)?, what is the graph of commensurate magnetism and superconductivity in cobalt-doped barium iron arsenide superconductor?, and etc. By developing a model Hamiltonian for the system and using diagonalized Bogoliubov transformation, We have found mathematical expressions for superconducting order parameter(Δsc) as a function of superconducting transition temperature(Tc), magnetic order parameter(Δ_{SDW}) as a function of spin density wave transition temperature (Tsdw), and spin density wave order parameter(Δ_{SDW}) as a function of superconducting transition temperature(Tc). The phase diagrams of superconducting transition temperature versus superconducting order parameter, spin density wave transition temperature versus spin density wave order parameter and superconducting transition temperature versus spin density wave order parameter have been plotted. By combining the two phase diagrams of spin density wave transition temperature versus spin density wave order parameter and superconducting transition temperature versus spin density wave order parameter, we have obtained a phase diagram which shows the possible coexistence of spin density wave and superconductivity in ($Ba(Fe_{1-x}Co_x)_2As_2$). The commensurate SDW order appears below the structural transition temperature and SC coexists with SDW order in under doped region. The commensurate SDW order changes into transversely incommensurate SDW order that coexists and competes with superconductivity. The coexistence phase between SC and (in) commensurate SDW orders does exist at lower superconducting transition temperature (Tc). The commensurate SDW order appears below the structural transition temperature and SC coexists with SDW order in under doped region. Near optimal superconductivity, it has been shown that the commensurate SDW order changes into transversely incommensurate SDW order that coexists and competes with superconductivity.

Table of Contents

ACKNOWLEDGMENTS iii

ABSTRACTS iv

1. INTRODUCTION 1

1.1 Background of the study 1

1.2 Statement of the problem 5

1.3 Objectives of the study 6

1.3.1 General Objectives 6

1.3.2 Specific Objectives 6

2. REVIEW OF RELATED LITERATURE 7

2.1. Iron Based Superconductor 7

2.2. ‘122’ Family Bases Superconductors 8

2.3. Crystal Structure and Magnetic Order for Iron-based superconductors 9

2.4 Commensurate SDW and Superconductivity 11

2.5 Phase Diagrams for Iron based Superconductors 13

2.6. Electron Doped Barium Iron Arsenide 14

2.7. Effectof Electron Doping 15

2.7.1 Parent compound 17

2.7.2. Under Doping 17

2.7.3. Optimal Doping 18

2.7.4. Over Doping 18

3. MATHEMATICAL TECHNIQUES 19

3.1 Model Hamiltonian 19

3.2 Coexistence of Commensurate SDW and Superconductivity in Ba $(Fe_{1-x}Co_x)_2$ As_2 superconductors 20

3.2.1. The Order Parameter of Superconductivity 20

3.2.2. The Order Parameter of Spin Density Wave (SDW) 25

3.2.3. The Order Parameter of Superconductivity and Spin Density Wave (SDW) 28

4. RESULT AND DISCUSSION 31

5. CONCLUSION 35

BIBLIOGRAPHY 36

Table of figures

Figure 1.1: Vanishing of electrical resistivity below a critical temperature Tc, discovered in mercury by KamerlinghOnnes in 1911 1

Figure 1.2: A comparison of the response of a perfect conductor and a superconductor to an applied magnetics field. 2

Figure 1.3: The formation of a cooper pair. 3

Figure 1.4: Phase diagram of type I and type II superconductors 3

Figure 1.5: Evolution of critical temperatures of superconducting materials with time 4

Figure 2.1: Five crystal structures of the iron-based superconductors 8

Figure 2.2: Schematic diagram illustrates the crystal structure of (Ba $(Fe_{1-x}Co_x)_2 As_2$) in the tetragonal state. 9

Figure 2.3:Diagram of the crystal structure of (Ba $(Fe_{1-x}Co_x)_2 As_2$) in the antiferromagnetic state and Crystal structure of the Ba122 parent compound 10

Figure 2.4 Schematic diagrams of Fermi surface nesting. 11

Figure 2.5 Example of a commensurate AFM order and an incommensurate AFM order. 12

Figure 2.6 Experimental phase diagram for (Ba $(Fe_{1-x}Co_x)_2 As_2$) showing commensurate (C) and incommensurate (IC) antiferromagnetic order below T_N. 13

Figure 2.7: Temperature T vs doping x phase diagram of 122 type Co doped $BaFe_2As_2$. 16

Figure 4.1 Phase diagram of superconducting order parameter (Δ_{SC}) vs. superconducting transition temperature (Tc) for (Ba $(Fe_{1-x}Co_x)_2 As_2$) superconductor 32

Figure 4.2 Phase diagram of magnetic order parameter (Δ_{SDW}) vs. magnetic transition temperature (T_{SDW}) for (Ba $(Fe_{1-x}Co_x)_2 As_2$) superconductor. 32

Figure 4.3 Phase diagram of magnetic order parameter (Δ_{SDW}) vs. superconducting transition temperature (Tc) and the transition between commensurate and incommensurate SDW phases for (Ba $(Fe_{1-x}Co_x)_2 As_2$) superconductor. 33

Figure 4.4: Diagram of superconducting transition temperature (Tc), magnetic transition temperature (T_{SDW}), versus magnetic order parameter (Δ_{SDW}). 33

Table 2.1: Spin Resonance Energies in the Co doped Fe-Pnictide. 17

CHAPTER 1

1. INTRODUCTION

1.1 Background of the study

Superconductivity is a phenomenon in which the electric resistivity suddenly drops to zero at a particular temperature i.e. at critical temperature Tc. It was first discovered in 1911[1] by Heike Kamerling Onnes and his collaborators. While studying the electrical resistance of mercury [2] at low temperatures, they observed that the resistance sharply dropped to zero at a temperature of4.2K

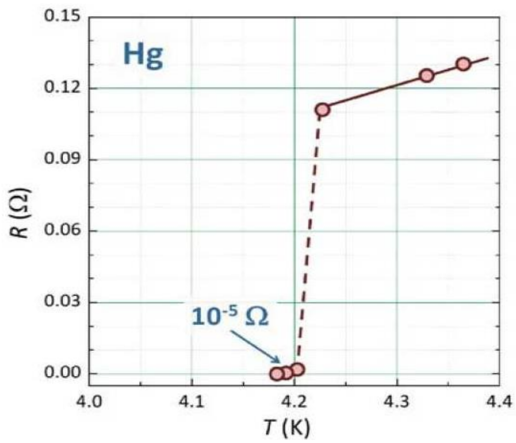

Figure 1.1: Vanishing of electrical resistivity below a critical temperature Tc, discovered in mercury by Kamerlingh Onnes in 1911. The image is taken from [3].

W. Meissner and R.Ochsenfeld (1933) discovered that when a superconductor is cooled below the transition temperature under an applied magnetics field, the applied field is excluded from the bulk of the superconductor, so that B = 0 throughout its interior [4], excluded by superconducting screening currents at the surface. This property of the superconducting state is known as the Meissner effect.

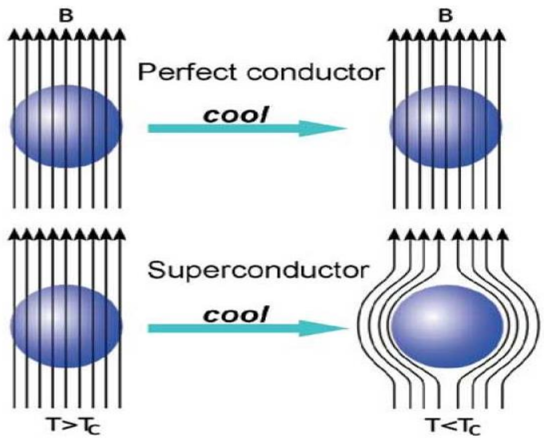

Figure 1.2: A comparison of the response of a perfect conductor and a superconductor to an applied magnetics field. When they are cooled below their critical temperatures, the magnetic field within the perfect conductor doesn't change, but the magnetic field within the superconductor is expelled (Meissner effect).

In1935, London theory was constructed by two brothers Fritz and Heinz London to understand the behavior of superconductors in electromagnetic field [5].

The Meissner effect does not cause the field to be completely ejected but instead the field penetrates the superconductor over a very small distance λ_L, called the London penetration depth, and is decaying exponentially to zero within the bulk of the material.

The first successful theory to explain the microscopic mechanisms of superconductivity was proposed by John Bardeen, Leon Cooper, and Robert Schrieffer in 1957[6, 7], now known as the BCS theory. The main point of the BCS theory is the formation of Cooper pairs. An electron moving through a conductor will attract nearby positive charges in the lattice. This deformation of the lattice causes another electron, with opposite momentum and spin, to move into the region of higher positive charge density. This looks like one electron attracts another electron through the lattice vibration, which can overcome the Coulomb repulsion, and then two electrons become correlated. Individual pairs are not stuck together forever. They are constantly breaking and reforming. Individual electrons cannot be identified, so rather than consider them to be dynamically changing pairs; they may be considered as permanently paired.

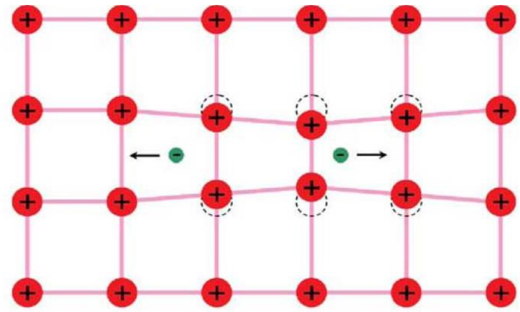

Figure 1.3: The formation of a cooper pair: A passing electron attracts the positive charged ions of the lattice, causing a slight ripple in its wake. Another electron passing in the opposite direction is attracted to that displacement.

Superconductors can be type I and type II according to their behavior in a magnetic field. In type I superconductors, when the strength of the applied field rises above the critical value the superconductivity abruptly destroyed. In type II superconductors, raising the applied field beyond a critical value Bc1 lead to a mixed state in which increasing amount of magnetic flux penetrates the material, but there remains no resistance to the flow of electrical current. At the second critical field Bc2, superconductivity is destroyed [54].

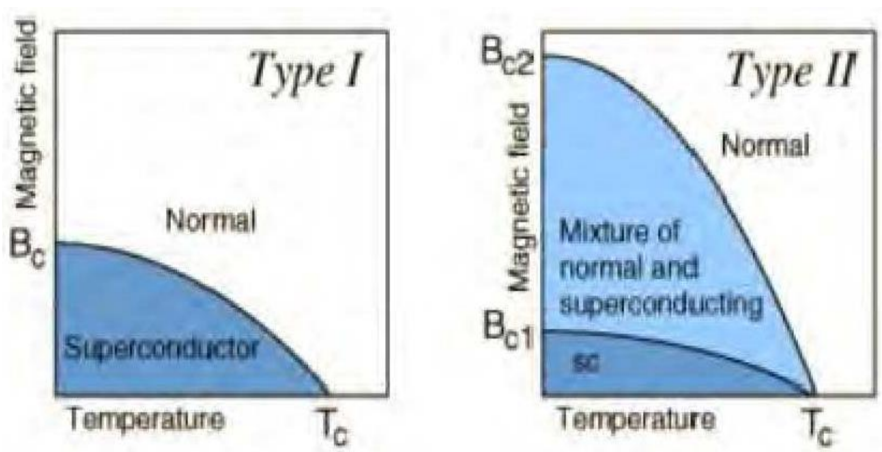

Figure1.4: Phase diagram of type I and type II superconductors

Copper-based superconductors discovered [8] in 1986 by Bednorz and muller. They discovered a lanthanum cuprate (LaBaCuO) superconductor with critical temperature 35K. Not much later, lanthanum was replaced by yttrium (YBaCuO), raising the critical temperature up to92 K. This was an important breakthrough because the now much cheaper liquid nitrogen could be used as a coolant. Liquid nitrogen has boiling point of 77 K at atmospheric pressure. Since then many new cuprates have been discovered.

For long time the cuprate dominated the field of high temperature superconductors. This changed in 2006 by Hideo Hosono and co-workers when superconductivity was found in an iron-based superconductor $LaFePO_{1-x}F_x$ at 4K [9]. But the iron-based superconductors gained much greater attention 2008 when a new iron-based superconductor $LaFeAsO_{1-x}F_x$ was found to superconductor at 26 K [10]. Moreover by applying pressure the critical transition temperature could be increased up to 43 K [11].Superconducting materials may be cast in two categories:

"Conventional" superconductors: Materials such as the elements, NbTi, and Nb_3Sn alloys.
"Unconventional" superconductors: Including the cuprate superconductors, heavy fermion superconductors (e.g. $CeCu_2Si_2$, $CeRhIn_5$, URu_2Si_2, etc.), some organic compounds (e.g. $La_{2-x}Sr_xCuO_4$, $YBa_2Cu_3O_7$, etc), and now the FeAs-based superconductors.

Hundreds of superconducting materials are known, including more than half of the known elements, a lot of intermetallic compounds, organic, spinel and perovskite compounds.

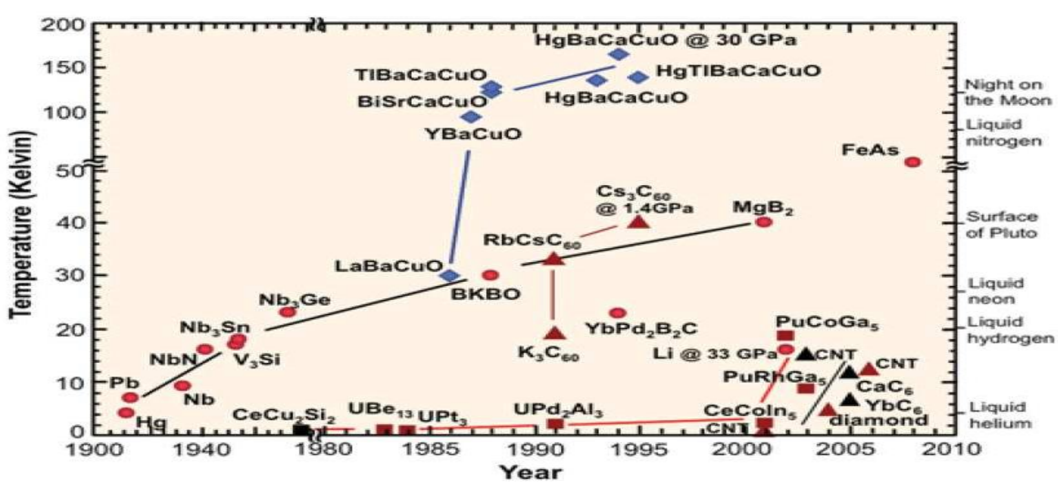

Figure 1.5: Evolution of critical temperatures of superconducting materials with time [12].

One century has passed since the discovery of superconductivity. During this period, many new superconductors were found and considerable progress in theory was made. Until now, superconductivity is one of the most actively studied field in the solid state physics and attracts immense experimental and theoretical efforts. Superconducting properties can make them useful for many possible industrial applications, such as making the magnets in magnetic resonate imaging machines (MRI), magnetic-levitated trains and power transmission without energy loss from heat. One obstacle of using these superconductors is that one needs to cool down the material to very low temperature, which has a high cost economically. Superconductors can conduct electricity without energy loss and thus have important applications. Under normal conditions (for example, at room temperature), metals such as aluminum and copper can conduct electricity, but they all have some electrical resistance. When a voltage is applied to a metal, electrons move in a certain direction and current forms. It is inevitable that a moving electron hits other objects, like impurities (no material is absolutely pure) or other electrons. Then the energy will be lost as these collisions convert electron energy into heat. Resistance is the quantity that characterizes the energy loss. Superconductors have exactly zeroed electrical resistance.

1.2 Statement of the problem

There were a number of problems in the study of superconductivity. Among those problems high temperature superconductivity is the principal.

- The study will be raises the following basic question.
- Why are the FeAs-based superconductors interesting to study?
- What is the effect of electron doped barium iron arsenide ($Ba(Fe_{1-x}Co_x)_2As_2$)?
- What is the phase diagram of cobalt doped barium iron arsenide ($Ba(Fe_{1-x}Co_x)_2As_2$)?
- What is the graph of commensurate magnetism and superconductivity in cobalt-doped barium iron arsenide superconductor ($Ba(Fe_{1-x}Co_x)_2As_2$)?
- What is crystal structure of cobalt doped barium iron arsenide ($Ba(Fe_{1-x}Co_x)_2As_2$)?

1.3 Objectives of the study

1.3.1 General Objectives

The major objective of this research was:

- To study the *commensurate magnetism and superconductivity in electron-doped barium iron arsenide super conductor* ($Ba(Fe_{1-x}Co_x)_2As_2$).

1.3.2 Specific Objectives

The research would be able to:

- Understand evolution of critical temperatures of superconducting materials with time.
- Develop the model Hamiltonian based on observing electronic structure in system.
- Obtain mathematical expressions of superconducting critical temperature, superconducting order parameter, the magnetic order parameter and transition temperature and also studying the relation between parameters from which we solve for transition temperature and doping parameter.
- Draw the graph, depending on the relation between superconducting critical temperature, superconducting order parameter, and the magnetic order parameter and transition temperature.

CHAPTER 2

2. REVIEW OF RELATED LITERATURE

2.1. Iron Based Superconductor

Iron-based superconductors started with the discovery of superconductivity at 4 K in LaFePO in 2006, and great interests have been drawn since 2008 when discovery by Hosono *et al.* of superconductivity in the electron-doped LaOFeAs (La1111) at 26 K [15]. Since then, enormous researches have been done on the materials, with Tc reaching as high as 55 K Critically important feature of the Fe-based superconductors is a material having finite conductivity as the absolute temperature T approaches zero kelvins [39].

There are various types of iron based superconductors, which can be divided into two major categories:

- Iron pnictides(P,As) and
- Iron chalcogenides(S, Se, Te).

These categories can be further divided into several families of compounds based on their chemical formulas and crystal structures. All structures of iron-based superconductors share a common layered structure based upon a planar layer of iron atoms joined by tetrahedrally coordinated pnictogen or chalcogen an ions arranged in a stacked sequence separated by alkali, alkaline earth or rare earth and oxygen/fluorine "blocking layers." The electronic properties of iron pnictides show a more metallic behavior than iron chalcogenides, and also suffer less from the disorder effect of iron interstitials or vacancies [13]. Iron-based superconductivity has been found in compounds like LnFeAsO (Ln=La,Ce,Nd,Pr,Sm...) and AFeAsF (A = Ba, Sr...), AFe_2As_2 (A=Ba,Sr...) and KFe_2Se_2, AFeAs (A=Li,...), FeSe(Te) and $Sr_4V_2O_6Fe_2As_2$[14]. It is now common to classify iron-based superconductors in to several structural families, dented shortly by the stoichiometric ratios of chemical constituents in their un doped parental compounds, “11” for binary iron-chalcogenide compounds like FeTe or FeSe, “111” for the originally discovered RFeAsO(R-rare earth), “122” for AFe_2As_2(A-alkali metal) and other[40].

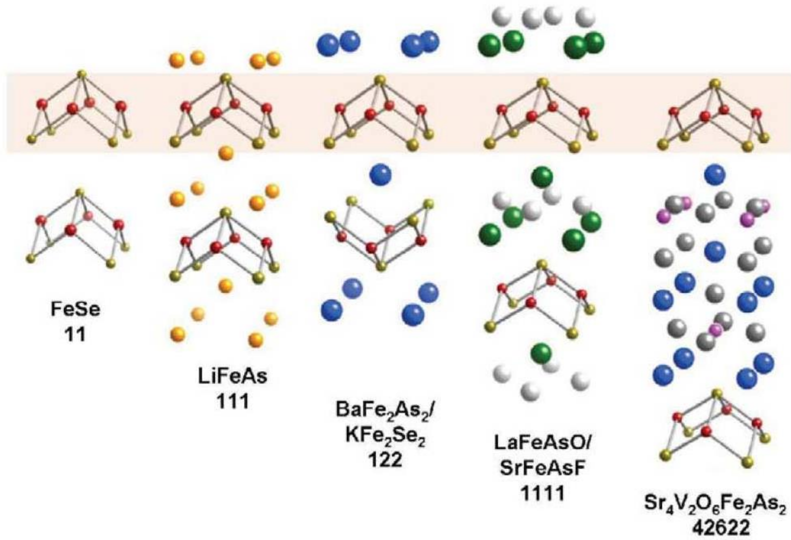

Figure 2.1: Five crystal structures of the iron-based superconductors. All these structures share a common layered structure based upon a planar layer of iron atoms(red) joined by tetrahedrally coordinated pnictogen (P, As) or chalcogen (S, Se, Te) anions(gold)[16].

2.2. '122' Family Bases Superconductors

The 122 family compounds have the well-known $ThCr_2Si_2$ type structure, the first member of this family, $BaFe_2As_2$ compound, was quickly discovered by Johrendt's group. The study of Fe-based superconductor is one of the most fruitful fields of present research in superconductivity. M. Rotter et al. proposed $BaFe_2As_2$ as a potential new parent compound based on the similarities between $BaFe_2As_2$ and LaFeAsO. There are several compounds of '122' Family Bases Superconductors. Among the 122 system, $BaFe_2As_2$ appears as the prototypical iron pnictide compound as superconductivity can be induced either by substitution on the iron site (electron doping by Co or Ni [17–19]; isovalent substitution by Ru [20, 21]), substitution on the Ba site (hole doping by potassium substitution [22]) or substitution on the As site (isovalent phosphorus substitution [23–25]) (more references can be found in the paper of Martinelli et al. [27]). This provides an exceptional playground to study the different modifications of the electronic structure and their consequences on the transport properties. Albeit less studied, all these substitutions are also possible in the $SrFe_2As_2$ family and display a lot of similarities with the behavior observed in the $BaFe_2As_2$ family. The most studied and probably the largest numbers of superconductors are in the 122 family which are made up of combination of metallic alkaline earth (Ba, K, Ca, Sr…) transitional metal (Fe,Co,Ni…) and pnictogen(As,P).

The nature of iron based superconductors surprises everyone (who knows it) by bringing together two incompatible phenomena, superconductivity and magnetism, into coexistence [41]. Due to this fact it attracted a lot of experimental interest and theoretical calculation of this age [42, 43]. The knowledge of superconducting mechanism in iron-based superconductors is very crucial to analyze the lattice structure, magnetic ordering, spin fluctuations and pairing mechanism of superconductors [44]. This is because of not only for with even higher transition temperature than cuprates but also they allow one to potentially understanding of the essential in gradient of high-temperature superconductivity [45].

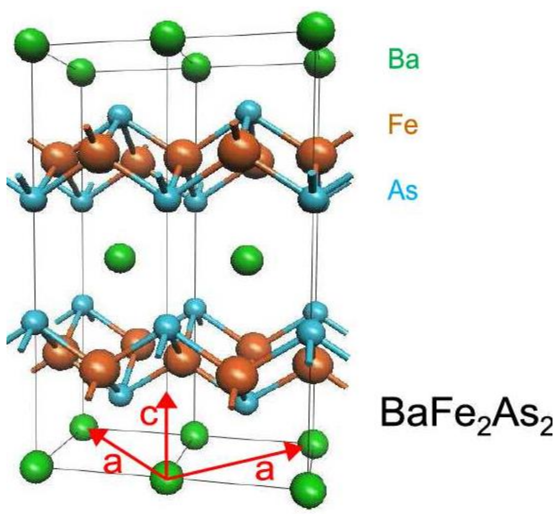

Figure 2.2: Schematic diagram illustrates the crystal structure of ($Ba(Fe_{1-x}Co_x)_2As_2$) *in the tetragonal state. Lattice vectors are shown by red arrows.*

2.3. Crystal Structure and Magnetic Order for Iron-based superconductors

Similar to cuprate materials, Iron-based superconductors crystallize in layered crystal structures. The parent compound $BaFe_2As_2$ consist of iron atoms sandwiched between arsenic atoms with barium filler layers in between fig 2.3a depicts the tetragonal $BaFe_2As_2$ unit cell. It consists of two iron-arsenic layers, with two iron and two atoms in each layer, and two barium atoms. As illustrated in figure 2.1 for the four main classes of Iron-based materials, these layered crystal structures are organized in an alternate stacking of Fe_2As_2-layers and layers containing the other elements of the composition. The only exception is the 11 family materials. Here, the Fe_2As_2 -layers are substituted by $Fe_2(Se/Te)_2$-layers, in the absence of additional buffer layers.

The orthorhombic unit cell is tetragonal rotated 45^o around the c-axis and stretched so the barium atoms create an FCC instead of the BCC seen in fig. 2.3b. The lattice constant for the parent compound is a=b=3.96Å and c=13.0Å [46] at room temperature.

When cooling $BaFe_2As_2$ it simultaneously under goes structural transition from tetragonal to orthorhombic and becomes AFM ordered. The magnet coupling is ferromagnetic in the (a,-b, 0) and antiferromagnetic in the (a, b, 0) and (0, 0, c) directions as displayed in figure 2.3a. The AFM ordering vector is QAFM= (12, 12, L) where L is odd [46].

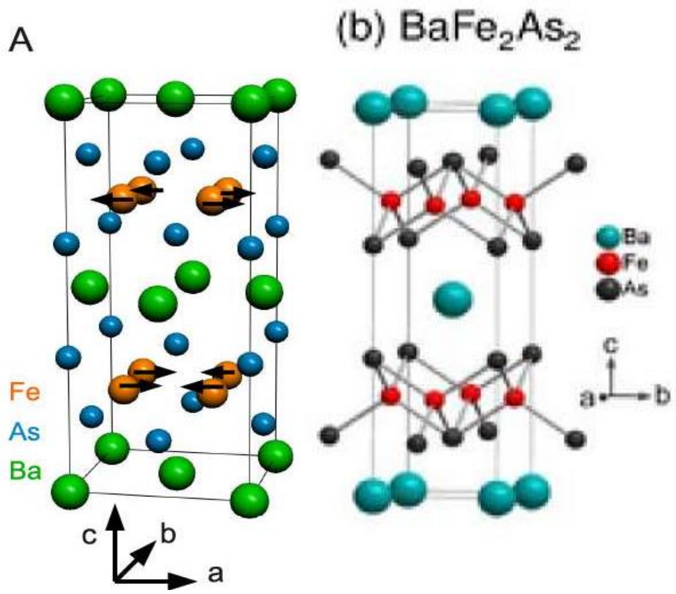

Figure 2.3: (A) Diagram of the crystal structure of ($Ba(Fe_{1-x}Co_x)_2As_2$) *in the antiferromagnetic state. The magnetic moments on the iron sites point in the a-direction, and align antiparallel along the longer a-axis, and parallel along the shorter b-axis. (B) Crystal structure of the Ba122 parent compound (space group I4/mm). Green is barium. Red is iron. Black is arsenic. The lattice parameters are: a axis is 3.9625 Ǻ, c axis is 13.0168 Ǻ, dFe−Fe 2.802 Ǻ, dFe−As 2.403 Ǻ. Cobalt doping will replace an iron atom. Figure reprinted from Rotter et al [64].*

Electronic and magnetic nematic degrees of freedom are believed to be associated with the origin of structural transitions and their interplay with magnetism in 122- systems.

Orbital ordering drives the structural transition and induces magnetic anisotropy, thus triggering the magnetic transition [29-31];

Magnetic fluctuations drive the structural transition and induce orbital ordering [32].

The structural transformation temperature Ts can be reliably ascertained by diffractometric analysis carried out as a function of temperature; in particular for 122-type compounds a selective Bragg peak splitting marks the symmetry breaking. Conversely, no anomaly can be detected on crossing Ts by optical measurements [33, 34], since no displacive optical mode is involved.

Since anti-ferromagnetism in the FeAs-based superconductors originates from conduction electrons that also form the Cooper pairs below Tc, it is intriguing that superconductivity and anti-ferromagnetism compete for the same electrons which were not expected, especially when it is known that the magnetism is generally detrimental for superconductivity.

2.4 Commensurate SDW and Superconductivity

The parent 122 compounds exhibit a commensurate SDW order. Taking one electron and one hole pocket, If the size of electron pocket (blue) and hole pocket (red) are the same, they nest perfectly as shown in Fig. 2.4 (a) and results in a commensurate SDW order with QAFM. When the shapes of electron and hole pockets are different but two pockets have the same size in one of the directions as in Fig. 2.4 (b), it still results in a commensurate AFM order. However, when the sizes of electron and hole pockets are different as in Figs. 2.4 (c) and (d), the nesting becomes imperfect with a commensurate SDW vector QAFM that causes a shift of the Fermi surface for more nesting and results in an incommensurate SDW order with τ = QAFM+~ε.

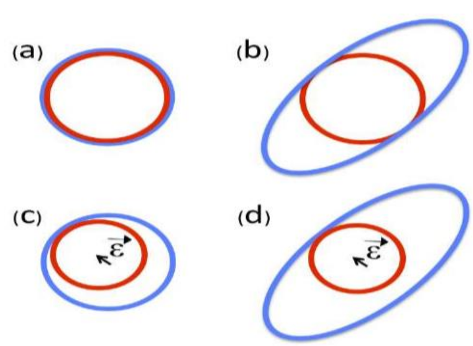

Figure 2.4 Schematic diagrams of Fermi surface nesting. Hole (red) pockets are shifted by QAFM. (a) Perfect nesting between electron (blue) and hole (red) pockets. (b) Imperfect nesting

due to different shapes of electron and hole pockets. In one direction (from lower-right to upper-left), both sides of electron and hole pockets are partially nested. (c) Imperfect nesting due to different sizes of electron and hole pockets. The hole pocket is shifted with ε for more nesting. (d) Imperfect nesting due to different sizes and shapes of electron and hole pockets. The hole pocket is shifted with ε for more nesting.

The directions of spins alter on each site but the periodicity (black solid line) matches with the periodicity in the crystallographic structure (red dashed line). One example of an incommensurate AFM order is that the varying magnitude of the spins (the periodicity) does not match with the periodicity of the crystallographic structure as in Fig. 2.5 (b).

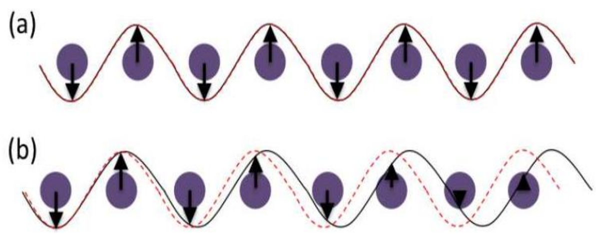

Figure 2.5 (a) Example of a commensurate AFM order. (b) Example of an incommensurate AFM order. The arrows indicate spin directions. The crystallographic (red dashed) and antiferromagnetic (balck solid) periodicities are displayed with sinusoidal lines. Two lines are overlaid in (a) but not in (b).

The nature of magnetism in under doped region in FebSCs is an intensively studied topic, due to its comp with superconductivity and the possible relation with the pairing mechanism. In the early time of discovery of FebSCs the nature of magnetic order had been in debate. Most recent studies have indicated the commensurate SDW order in several systems including the parent compounds and doped compounds. The reports support the idea that superconductivity in iron based materials can be induced via electron or hole doping or pressure. Experiments on doped Ba122 FebSCs confirm that the commensurate SDW order appears below the structural transition temperature and SC coexists with SDW order in under doped region. Although these results indicate that the static SDW order competes with SC, it remains unclear during the discovery whether the SDW order truly coexists microscopically with superconducting regions.

Near optimal superconductivity, it has been shown that the commensurate SDW order changes into transversely incommensurate SDW order that coexists and competes with superconductivity.

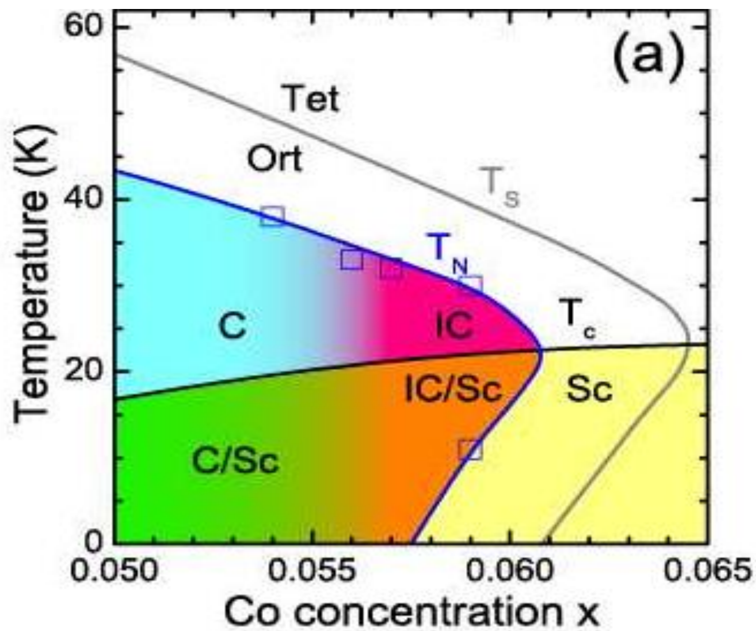

Figure 2.6 Experimental phase diagram for (Ba ($Fe_{1-x}Co_x$) $_2$ As_2) *showing commensurate (C) and incommensurate (IC) antiferromagnetic order below* T_N. *Tetragonal (Tet) and orthorhombic (Ort) phases are separated by the phase line at TS. Superconductivity (SC) appears below Tc and can coexist with both commensurate (C/SC) and incommensurate (IC/SC) magnetic order.*

The nematic and orbital fluctuations are being observed at the phase boundary between the magnetic and SC phases in some FebSCs. This case has been considered experimentally and the conclusion was that the transition from the SDW to SC phase is always of first order, regardless of shapes of the Fermi pockets or the shift of chemical potentials.

2.5 Phase Diagrams for Iron based Superconductors

The magnetic order sets in after the crystal structure has made a transition from tetragonal to orthorhombic symmetry. In the 11-materials both phase transitions, magnetic and structural, occur simultaneously at the same temperature whereas for the 122-class the two transitions start to separate for higher doping concentrations. For 1111-class even the un doped materials exhibit a temperature difference of up to 20K between the structural and magnetic transition. Doping the system with foreign atoms is one method to suppress the magnetic order and eventually induce superconductivity to the system. The doping can be conducted in several different ways, as basically all elements of the material can be replaced by foreign atoms. Depending on the introduction of these foreign atoms, they absorb or emit electrons from or to the system. Thus, the doping is referred to as either hole- or electron-doping. Increased doping concentration leads to a continuous suppression of the magnetic and nuclear transition temperatures which is accompanied by a continuous reduction of the ordered magnetic moment and orthorhombic distortion of the crystal structure. As soon as the long range order is suppressed, the system becomes superconducting and aside for a small phase present in 122-families the superconducting phase is related to a tetragonal crystal structure

2.6. Electron Doped Barium Iron Arsenide

The highest Tc is achieved when magnetism is completely destroyed or at least strongly hindered; this can usually be obtained by electron- or hole-doping, but in some cases superconductivity can also emerge by applying pressure.

Barium Iron Arsenide can be electron doped by Co and Ni $Ba(Fe_{1-x}(Co, Ni)_x)_2As_2$.Iron is ferromagnetic transitional metal whose electronic confugration is Fe:$3d^6 4s^2$[47]. The iron 3d eectrons are responsible for the low laying electronic structure [48] and this 3d electrons are the conduction electrons[49]. The electron play a big role in superconductivity[50]. The study for the iron-based superconductivity is one of the particular interast becouse Fe^{2+} ions have magnetic moments wich are generally believed to be detrimental to superconductivity, and the discovery of high- Tc superconductivity in iron pnictides has over turned this view point and opens a new directions for exploring new superconductors [51]. Compare to Fe^{2+} ion, Co^{2+} ($3d^7$) has one more 3d electrons, but Ni^{2+} ion ($3d^8$) has two more electrons. Then it is expected that each Ni dopant induces two extera itinerant electrones while each Co dopant only induces one extra itinerant electron. Thus the fact that the optimal doping contant of Ni is only about half of that of Co can be understood. Actually both Ni doped and Co doped system show muxmum Tc at the same effective doping level [52]. A discovary of suerconductivity in $BaFe_2As_2$ under electron doping , by substitution of Fe atoms by Co and Ni forming $Ba(Fe_{1-x}(Co,Ni)_x)_2As_2$ has been at low cobalt and nickel concentrations.

2.7. Effect of Electron Doping

One of the ways of achieving superconductivity in FebSC materials is via electron/hole doping. In the undoped state, the 122 compound exhibits simultaneous structural and magnetic phase transitions below 140K, changing from the high temperature paramagnetic tetragonal phase to the low temperature orthorhombic phase with the collinear AFM structure. On electron doping on 122FebSCfamilies the static AFM order is suppressed and superconductivity emerges [39]. From magnetic measurements of single crystals the phase diagram for Co-Ba122 was established, where the single structural/magnetic phase transition in Ba122 splits with increasing Co doping. Neutron diffraction experiments on Co-Ba122 confirm that the commensurate AFM order appears below the structural transition temperature and superconductivity coexists with AFM order for $0.06 \leq x \leq 0.102$.

Neutron scattering and other experiments on electron doped 122 FebSCs confirmed that commensurate long range AFM coexist with SC in under doped region. In addition, for electron doped Ba122 samples near optimal SC, it has been shown that the commensurate static AFM order changes into transversely incommensurate short range AFM order that coexists and competes with superconductivity. For the under doped regime commensurate AFM order seems to microscopically coexist with superconductivity in hole doped 122 compound short range incommensurate AFM order in K-Ba122 near optimal superconductivity.

Barium has electron configuration $[Xe]6s^2$ which favor the Ba^{2+} state, arsenic which the electron configuration $[Ar]3d^{10}4s^24p3$favors As^{3-}, which means iron is in the Fe^{2+} state with the electron configuration $[Ar]3d^6$ and give 6 electrons to the conducting band. There are several ways to dope $BaFe_2As_2$. In hole doping you can replace Ba^{2+} with K^+ which gives away one less electron/creates an extra hole. When you doped $BaFe_2As_2$ with cobalt you replace the Fe^{2+} ion with the electron configuration $[Ar]3d^7$ which has an extra conducting electron in the d-sell. The extra electron (holes) the possibility for the electron to pair up and superconductivity can emerges [53]. An important step to understand superconductivity in Fe-pnictde system is the determination of the phase diagram as function of doping [66]. A typical phase diagram of an iron based superconductor in the (T,x) plane, where x upon doping , the spin density wave order parameter is suppressed and show a metallic antiferromagnetic order, also called spin density wave, below T_N at x=0[56]. A unique feature associated with the magnetism of this compound is structural phase transition (T=Ts) from the high temperature tetragonal phase to the low temperature orthorhombic phase which always precedes the magnetic ordering (T_S>T_N) as shown in figure below. Iron arsenide superconductors present a very rich phase diagram displaying superconducting, anti-ferromagnetic and structural order [57].

Iron substitutions by atoms situated at the right of iron in the periodic table are expected to electron dope the system. This was clearly evidenced by ARPES measurements [35, 36] which showed that the areas of the hole bands decrease and those of the electron bands increase upon Co substitution, contrary to some theoretical proposals [37]. Moreover as shown in Fig. 2.6, the phase diagrams for these substitutions match with each other if they are plotted as a function of electron doping, showing unambiguously that each Co atom adds one electron to the bands. When $BaFe_2As_2$ is doped by cobalt, the temperature of the SDW transition is observed to decrease and the SDW eventually disappears completely as the amount of dopant is increased.

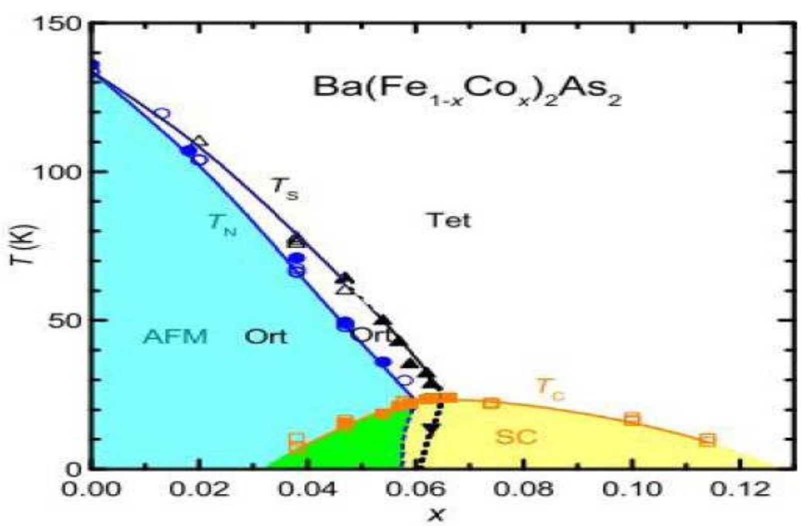

Figure 2.7: Temperature T vs doping x phase diagram of 122 type Co doped ($Ba(Fe_{1-x}Co_x)_2As_2$).

Actually, in $BaFe_2As_2$, the systematic substitution of either the alkaline earth (Ba), transition metal (Fe) or pnictogen (As) atom with a different element almost universally produces a similar phase diagram as ($Ba(Fe_{1-x}Co_x)_2As_2$).

Table: 2.1. Spin Resonance Energies in the Co doped Fe-Pnictide

Compound	Doping level(%)	Sample	Tc(K)	Resonance Energy(meV)	Er/kBTc	Ref.
Ba $Fe_{2-x}Co_x$ As_2	x=4%	Self-flux	11	4.5	4.9	A
	x=4.7%	Self-flux	17	~ 4.5	3.2	B
	x=5.4%	Self-flux	23	~ 10	5.2	C
	x=6.8%	Self-flux	22.2	8.3	4.5	D
	x=7.5%	Self-flux	25 25	9.5 9.6, 10.5*	4.6 4.6, 5.0	E F
	x=8%	Self-flux	22	8.6	4.7	G

* Resonances at two wave vectors – ½, ½, 1 and ½, ½, 0 - with different energies.[a] Christianson et al. (2009), [b] Pratt et al. (2009),[c] Lester et al. (2010), [d] H.-F. Li et al. (2010), [e] Inosov et al. (2010), [f] Park et al. (2010), [g] Lumsden et al. (2009),

2.7.1 Parent compound

Parent compound are compounds without pressure or doping. The parent compound has no superconducting transition and the curvatures suggest a normal Fermi-liquid behavior. Nevertheless, there is quite some physics going on. At around 130 K the resistivity drops suddenly, identified as the magnetic or spin density wave (SDW) transition [58]. The transition coincides with a structural transition from a high temperature tetragonal- to a low temperature orthorhombic- crystal structure. From literature [59, 58, 60, 61] it is known that cobalt doping lowers the SDW transition temperature, hence the assumption is made that the sample with the highest SDW transition also the most pure parent compound.

2.7.2. Under Doping

The crystals grown with the lowest doping levels are the x = 0.03 doped samples. These under doped crystals have a SDW and structural transition, only now they are shifted to lower temperatures and separated by almost 10 K. [62]

The next doping level is the Ba122 crystal with x = 0.04. Surprisingly, these crystals are from the same batch as x = 0.03(Co). This was unknown at the time of the measurement, and only after EMPA measurements it became clear that, for these low doping levels, apparently, the crystals outside of the crucible have a substantial higher Co concentration than the crystals inside.

2.7.3. Optimal Doping

These doping levels have the highest Tc, hence called optimal doped. Superconductivity emerges with maximum $T_{c(x)}$ near the point where $T_{c(x)}$ exceeds $T_{N(x)}$ ("an optimal doping")[63]. The first crystals grown by our own crystal grower Dr. Y. Huang, had a nominal cobalt doping of x = 0.07. The optimal Co concentration was known from literature to lie around x = 0.07. However, the actual Co concentration in the crystals was unknown at the time of the measurement. Also, the flux crystal grow conditions were changed by the principal of trial-and-error. As a consequence, there are a lot of different batches with different real cobalt concentrations. After all batches were measured with EPMA it is found that the nominal x = 0.07 batches could be roughly divided in two real doping levels, x = 0.071 and x = 0.073. The x = 0.071 all have reasonable high Tc's, around 23 K.

2.7.4. Over Doping

These batches have higher cobalt concentrations than the optimally doped crystals. By increasing the cobalt concentration the superconducting transition temperature is lowered or ultimately completely suppressed, hence these crystals are called over-doped [62].Now we are only left with two extremely over-doped batches, x = 0.10 and x = 0.11of Co concentration. The cobalt concentrations are now so high that the superconducting transition is completely suppressed. Unfortunately, almost all these crystals show a downturn at low temperatures.

CHAPTER 3

3. MATHEMATICAL TECHNIQUES

In this chapter, we derive the equation of motion using mathematical techniques that is used to drive gap equation to calculate the magnetic and superconductor parameter.

There are different types of mathematical methods such as the Bogoliubov transformation, Green function, the Hubbard model, Stoner model etc. In this work, we used the diagonalized Bogoliubov transformation to obtain the expressions of the magnetic and superconductor parameter.

3.1 Model Hamiltonian

We can develop the Hamiltonian for coexistence of Commensurate SDW and Superconductivity state from those of each independent state (Sc and SDW states).In developing the Hamiltonian we consider a multiband model nature of FebSC compounds as an itinerant metal containing electron bands at the center of unfolded Brillouin zones. The full mean field Hamiltonian for a system with intertwined SC and SDW order is given by

$$H = H_1 + H_2 + H_3.$$

$$H_1 = \sum_{k,\delta} (\epsilon_k - \mu)\, C^{\dagger}_{k\delta} C_{k\delta}.$$

$$H_2 = \sum_{kk'} V_{kk'}\; C^{\dagger}_{k\uparrow} C^{\dagger}_{-k\downarrow} C_{-k'\downarrow} C_{k'\uparrow} \tag{1}$$

$$H_3 = \sum_{KK'\sigma} V^{SDW}_{KK',\sigma} C^{\dagger}_{K,\sigma} C_{K+q,\sigma} C^{\dagger}_{k'+q,\bar{\sigma}} C_{K',\bar{\sigma}}$$

Here, $C^{\dagger}_{k\delta}$ creates an electron with momentum k and spin δ, and we already included the chemical potential by defining $\xi_k = \epsilon_k - \mu$

ξ_k is free electron energy , $\epsilon_k = \frac{\hbar^2 k^2}{2me}$ and $V_{kk'}$ is the interaction potential between electrons of a cooper pair.

3.2 Coexistence of Commensurate SDW and Superconductivity in Ba $(Fe_{1-x}Co_x)_2$ As_2 superconductors

In Co doped $BaFe_2As_2$, we have coexistence of commensurate SDW and superconductivity. In this case, superconducting mechanism is attributed to a strong coulomb interaction of the electron in the system, which can also be the cause for appearance of SDW state. And this suggest that the existence of competition between the two state. In his section we want to drive an expression for the order parameters of commensurate SDW, Δ_{SDW} and order parameters of superconductivity, Δ_{SDW} , as function of both of them, and temperature and to compare the variation of each with temperature.

3.2.1. The Order Parameter of Superconductivity

In this section we drive an expression for superconducting parameter by using Bogoliubov transformation.

$$\hat{H}_{SC} = H_1 + H_2 \quad and$$

$$\hat{H}_{SDW} = \hat{H}_3 \tag{2}$$

Therefore

$$\hat{H}_{SC} = \sum_{k,\delta} \xi_k\, C^\dagger_{k\delta} C_{k\delta} + \sum_{kk'} V^S_{kk'}\, C^\dagger_{k\uparrow} C^\dagger_{-k\downarrow} C_{-k'\downarrow} C_{k'\uparrow} \tag{3}$$

The second term describes the destruction of cooper pair (two electrons with opposite momentum [k,k'] and spin [$\uparrow,\downarrow$]) and the subsequent creation of cooper pair.

To decouple the Hamiltonian we use the mean field approximation. To proceed, we perform the usual mean-field decoupling of the quartic term.

$$\langle C^\dagger_{k\uparrow} C^\dagger_{-k\downarrow} C_{-k'\downarrow} C_{k'\uparrow}\rangle = \langle C^\dagger_{k\uparrow} C^\dagger_{-k\downarrow}\rangle C_{-k'\downarrow} C_{k'\uparrow} + C^\dagger_{k\uparrow} C^\dagger_{-k\downarrow}\langle C_{-k'\downarrow} C_{k'\uparrow}\rangle - \langle C^\dagger_{k\uparrow} C^\dagger_{-k\downarrow}\rangle\langle C_{-k'\downarrow} C_{k'\uparrow}\rangle \tag{4}$$

When we substitute equation (4) in to equation (3) it becomes:

$$\hat{H}_{SC} = \sum_{k,\delta} \xi_k\, C^\dagger_{k\delta} C_{k\delta} + \sum_{kk'} V^{Sc}_{kk'}\, \langle C^\dagger_{k\uparrow} C^\dagger_{-k\downarrow}\rangle C_{-k'\downarrow} C_{k'\uparrow} + C^\dagger_{k\uparrow} C^\dagger_{-k\downarrow}\langle C_{-k'\downarrow} C_{k'\uparrow}\rangle$$
$$-\langle C^\dagger_{k\uparrow} C^\dagger_{-k\downarrow}\rangle\langle C_{-k'\downarrow} C_{k'\uparrow}\rangle \tag{5}$$

The mean value $\langle C^\dagger_{k\uparrow} C^\dagger_{-k\downarrow}\rangle$ is note zero, since it corresponds to one cooper pair in the superconducting state and the mean field Hamiltonian of superconducting state, expressed as:

$$\hat{H}_{SC} = \sum_{k,\delta} \xi_k \, C_{k\delta}^{\dagger} C_{k\delta} - \sum_{k} \left(\Delta_{SC} C_{k\uparrow}^{\dagger} C_{-k\downarrow}^{\dagger} + \Delta_k^{*} C_{-k\downarrow} C_{k\uparrow} \right) + \sum_{k} \Delta_k \langle C_{k\uparrow}^{\dagger} C_{-k\downarrow}^{\dagger} \rangle \qquad (6)$$

Where the mean field is:

$$\Delta_{SC} = -\sum_{kk'} V_{kk'}^{SC} \langle C_{-k'\downarrow} C_{k'\uparrow} \rangle \qquad (7)$$

3.2.1.1. Bogoliubov Transformation in Superconductivity

To solve the above equation, we use Bogoliubov Transformation. In particular, we define new fermionic operators $\gamma_{k\sigma}$ and coefficients: u_k , v_k

$$C_{k\uparrow} = u_k^{*} \gamma_{k\uparrow} + v_k \gamma_{-k\downarrow}^{\dagger} \qquad (8)$$

$$C_{-k\downarrow}^{\dagger} = u_k \gamma_{-k\downarrow}^{\dagger} - v_k^{*} \gamma_{k\uparrow}$$

Where $\gamma_{k\sigma}$ are the new fermionic operators given in terms of electronic creation and annihilation operators (σ=($\uparrow,\downarrow$) spin orientations) u_k , v_k are the complex coefficients.

In order for the fermionic commutation relation to be satisfied, the normalization condition:

$$|u_k|^2 + |v_k|^2 = 1 \qquad (9)$$

Must be satisfied. Substituting in the effective Hamiltonian yields:

$$\sum_{k,\delta} \xi_k \, C_{k\delta}^{\dagger} C_{k\delta} = \sum_{k} \xi_k \left[C_{k\uparrow}^{\dagger} C_{k\uparrow} + C_{-k\downarrow}^{\dagger} C_{-k\downarrow} \right]$$
$$= \sum_{k} \xi_k \left[(|u_k|^2 - |v_k|^2) \left(\gamma_{k\uparrow}^{\dagger} \gamma_{k\uparrow} + \gamma_{-k\downarrow}^{\dagger} \gamma_{-k\downarrow} \right) + 2|v_k|^2 + 2 u_k v_k \gamma_{k\uparrow}^{\dagger} \gamma_{-k\downarrow}^{\dagger} + 2 u_k^{*} v_k^{*} \gamma_{-k\downarrow} \gamma_{k\uparrow} \right]$$

As well as

$$-\sum_{k} \left(\Delta_{SC} C_{k\uparrow}^{\dagger} C_{-k\downarrow}^{\dagger} + \Delta_{SC}^{*} C_{-k\downarrow} C_{k\uparrow} \right)$$
$$= \sum_{k} \left[(\Delta_{SC} u_k v_k^{*} + \Delta_{SC}^{*} u_k^{*} v_k) \left(\gamma_{k\uparrow}^{\dagger} \gamma_{k\uparrow} + \gamma_{-k\downarrow}^{\dagger} \gamma_{-k\downarrow} \right) - (\Delta_{SC} u_k v_k^{*} + \Delta_{SC}^{*} u_k^{*} v_k) \right]$$
$$- \sum_{k} \left[(\Delta_{SC} u_k^2 - \Delta_{SC}^{*} v_k^2) \gamma_{k\uparrow}^{\dagger} \gamma_{-k\downarrow}^{\dagger} + (\Delta_{SC}^{*} (u_k^{*})^2 - \Delta_{SC} (u_k^{*})^2) \gamma_{-k\downarrow} \gamma_{k\uparrow} \right] \qquad (10)$$

Therefore, the effective Hamiltonian becomes:

$$\hat{\mathrm{H}}_{SC} = \sum_k \xi_k \left[(|u_k|^2 - |v_k|^2)\left(\gamma_{k\uparrow}^\dagger \gamma_{k\uparrow} + \gamma_{-k\downarrow}^\dagger \gamma_{-k\downarrow}\right) + 2|v_k|^2 + 2u_k v_k \gamma_{k\uparrow}^\dagger \gamma_{-k\downarrow}^\dagger + 2u_k^* v_k^* \gamma_{-k\downarrow}\gamma_{k\uparrow}\right]$$
$$+ \sum_k \left[(\Delta_{SC} u_k v_k^* + \Delta_{SC}^* u_k^* v_k)\left(\gamma_{k\uparrow}^\dagger \gamma_{k\uparrow} + \gamma_{-k\downarrow}^\dagger \gamma_{-k\downarrow}\right) - (\Delta_{SC} u_k v_k^* + \Delta_{SC}^* u_k^* v_k)\right]$$
$$- \sum_k \left[(\Delta_{SC} u_k^2 - \Delta_{SC}^* v_k^2)\gamma_{k\uparrow}^\dagger \gamma_{-k\downarrow}^\dagger + (\Delta_{SC}^* (u_k^*)^2 - \Delta_{SC} (u_k^*)^2)\gamma_{-k\downarrow}\gamma_{k\uparrow}\right]$$
$$+ \sum_k \Delta_{SC} \langle \mathrm{C}_{k\uparrow}^\dagger \mathrm{C}_{-k\downarrow}^\dagger \rangle$$
$$\hat{\mathrm{H}}_{SC} = \sum_k \left[2\xi_k |v_k|^2 - \Delta_{SC} u_k v_k^* - \Delta_{SC}^* u_k^* v_k + \Delta_{SC} \langle \mathrm{C}_{k\uparrow}^\dagger \mathrm{C}_{-k\downarrow}^\dagger \rangle\right]$$
$$+ \sum_k [\xi_k (|u_k|^2 - |v_k|^2) + \Delta_{SC} u_k v_k^* + \Delta_{SC}^* u_k^* v_k]\left(\gamma_{k\uparrow}^\dagger \gamma_{k\uparrow} + \gamma_{-k\downarrow}^\dagger \gamma_{-k\downarrow}\right)$$
$$+ \sum_k [2\xi_k u_k v_k - \Delta_k u_k^2 + \Delta_{SC}^* v_k^2]\left(\gamma_{k\uparrow}^\dagger \gamma_{-k\downarrow}^\dagger\right) + h.c \qquad (11a)$$

The effective Hamiltonian can be written in the form of:

$$\hat{\mathrm{H}}_{SC} = \hat{\mathrm{H}}_0 + \hat{\mathrm{H}}_1 + \hat{\mathrm{H}}_2 \qquad (11b)$$

With

$$\hat{\mathrm{H}}_0 = \sum_k \left[2\xi_k |v_k|^2 - \Delta_{SC} u_k v_k^* - \Delta_{SC}^* u_k^* v_k + \Delta_{SC} \langle \mathrm{C}_{k\uparrow}^\dagger \mathrm{C}_{-k\downarrow}^\dagger \rangle\right]$$

$$\hat{\mathrm{H}}_1 = \sum_k [\xi_k (|u_k|^2 - |v_k|^2) + \Delta_{SC} u_k v_k^* + \Delta_{SC}^* u_k^* v_k]\left(\gamma_{k\uparrow}^\dagger \gamma_{k\uparrow} + \gamma_{-k\downarrow}^\dagger \gamma_{-k\downarrow}\right)$$

$$\hat{\mathrm{H}}_2 = \sum_k [2\xi_k u_k v_k - \Delta_{SC} u_k^2 + \Delta_{SC}^* v_k^2]\left(\gamma_{k\uparrow}^\dagger \gamma_{-k\downarrow}^\dagger\right) + h.c \qquad (12)$$

Where “h.c.”; denotes the Hermitian conjugate. To diagonalize the Hamiltonian, we must find the coefficients, "u_k,v_k" that make the undesired term H_2 vanish. Hence, we obtain the quadratic equation:

$$2\xi_k u_k v_k - \Delta_{SC} u_k^2 + \Delta_{SC}^* v_k^2 = 0 \qquad (13)$$

Solving for the ratio v_k/u_kyields:

$$\frac{v_k}{u_k} = \frac{\sqrt{\xi_k^2 + |\Delta_{SC}|^2} - \xi_k}{\Delta_{SC}^*} \qquad (14)$$

Using the normalization condition of equation (9) we have:

$$|u_k|^2 + |v_k|^2 = 1$$

$$|u_k|^2 = \frac{1}{1+\left|\frac{v_k}{u_k}\right|^2} = \frac{1}{2}\frac{|\Delta_{SC}|^2}{\xi_k^2 + |\Delta_{SC}|^2 - \xi_k\sqrt{\xi_k^2 + |\Delta_{SC}|^2}}$$

$$|u_k|^2 = \frac{1}{2}\frac{|\Delta_{SC}|^2\left(\sqrt{\xi_k^2 + |\Delta_{SC}|^2} + \xi_k\right)}{\left(\sqrt{\xi_k^2 + |\Delta_{SC}|^2}\right)(\xi_k^2 + |\Delta_{SC}|^2 - \xi_k^2)}$$

$$|u_k|^2 = \frac{1}{2}\left(1 + \frac{\xi_k}{\sqrt{\xi_k^2 + |\Delta_{SC}|^2}}\right) \tag{15}$$

From which follows:

$$|v_k|^2 = \frac{1}{2}\left(1 - \frac{\xi_k}{\sqrt{\xi_k^2 + |\Delta_{SC}|^2}}\right) \tag{16}$$

It is convenient to define the excitation energy:

$$E_1(1) = \sqrt{\xi_k^2 + |\Delta_{SC}|^2} \tag{17}$$

Using the above relations, we obtain:

$$\hat{\mathrm{H}}_1 = \sum_k [\xi_k(|u_k|^2 - |v_k|^2) + \Delta_{SC}u_k v_k^* + \Delta_{SC}^* u_k^* v_k]\left(\gamma_{k\uparrow}^\dagger \gamma_{k\uparrow} + \gamma_{-k\downarrow}^\dagger \gamma_{-k\downarrow}\right)$$

$$\hat{\mathrm{H}}_1 = \sum_k \left[\frac{\xi_k^2}{\sqrt{\xi_k^2 + |\Delta_{SC}|^2}} + \left(1 + \frac{\xi_k}{\sqrt{\xi_k^2 + |\Delta_{SC}|^2}}\right)\left(\sqrt{\xi_k^2 + |\Delta_{SC}|^2} - \xi_k\right)\right]\left(\gamma_{k\uparrow}^\dagger \gamma_{k\uparrow} + \gamma_{-k\downarrow}^\dagger \gamma_{-k\downarrow}\right)$$

$$\hat{\mathrm{H}}_1 = \sum_k \sqrt{\xi_k^2 + |\Delta_{SC}|^2}\left(\gamma_{k\uparrow}^\dagger \gamma_{k\uparrow} + \gamma_{-k\downarrow}^\dagger \gamma_{-k\downarrow}\right)\hat{\mathrm{H}}_1$$
$$= \sum_{k\sigma} E_1(K)\gamma_{k\sigma}^\dagger \gamma_{k\sigma} \tag{18}$$

As well as

$$\hat{\mathrm{H}}_0 = \sum_k \left[2\xi_k|v_k|^2 - \Delta_{SC}u_k v_k^* - \Delta_{SC}^* u_k^* v_k + \Delta_{SC}\langle \mathrm{C}_{k\uparrow}^\dagger \mathrm{C}_{-k\downarrow}^\dagger\rangle\right]$$

$$\hat{\mathrm{H}}_0 = \sum_k \left[\left(\xi_k - \frac{\xi_k^2}{\sqrt{\xi_k^2 + |\Delta_{SC}|^2}}\right) - \left(1 + \frac{\xi_k}{\sqrt{\xi_k^2 + |\Delta_{SC}|^2}}\right)\left(\sqrt{\xi_k^2 + |\Delta_{SC}|^2} - \xi_k\right) + \Delta_{SC}\langle \mathrm{C}_{k\uparrow}^\dagger \mathrm{C}_{-k\downarrow}^\dagger\rangle\right]$$

$$\hat{H}_0 = \sum_k \left(\xi_k - \sqrt{\xi_k^2 + |\Delta_{SC}|^2} + \Delta_{SC} \langle C_{k\uparrow}^\dagger C_{-k\downarrow}^\dagger \rangle \right)$$

$$\hat{H}_0 = \sum_k \left(\xi_k - E_k + \Delta_{SC} \langle C_{k\uparrow}^\dagger C_{-k\downarrow}^\dagger \rangle \right) \tag{19}$$

Therefore, the effective Hamiltonian is:

$$\hat{H}_{SC} = \sum_{k\sigma} E_1(k) \gamma_{k\sigma}^\dagger \gamma_{k\sigma} + \sum_k \left(\xi_k - E_k + \Delta_k \langle C_{k\uparrow}^\dagger C_{-k\downarrow}^\dagger \rangle \right)$$

$$\hat{H}_{SC} = \sum_{k\sigma} E_1(k) \gamma_{k\sigma}^\dagger \gamma_{k\sigma} + E_0 \tag{20}$$

Where $E_0$is just the ground-state energy:

$$E_0 = \sum_k \left(\xi_k - E_1(k) + \Delta_k \langle C_{k\uparrow}^\dagger C_{-k\downarrow}^\dagger \rangle \right) \tag{21}$$

Note from Eq. (8) that a Bogoliubon$\left(\gamma_{k\sigma}^\dagger\right)$ is a mixture of electrons and holes:

$$\gamma_{k\uparrow} = u_k C_{k\uparrow} - v_k C_{-k\downarrow}^\dagger$$

$$\gamma_{-k\downarrow} = u_k^* C_{-k\downarrow}^\dagger + v_k^* C_{k\uparrow} \tag{22}$$

3.2.1.2. The Gap Equation

We still need to determine the gap functionΔ_{SC}, given self-consistently by Eq. (7). Using the Bogoliubov transformation (8), we have:

$$\Delta_{SC} = -\sum_{k'} V_{kk'}^{SC} \, \langle \left(u_{k'}^* \gamma_{-k'\downarrow} - v_{k'} \gamma_{k'\uparrow}^\dagger \right) \left(u_{k'}^* \gamma_{k'\uparrow} + \gamma_{-k'\downarrow}^\dagger \right) \rangle$$

$$\Delta_{SC} = -\sum_{k'} V_{kk'}^{SC} \, u_{k'}^* v_{k'} \left(\langle \gamma_{-k'\downarrow} \gamma_{-k'\downarrow}^\dagger \rangle - \langle \gamma_{k'\uparrow}^\dagger \gamma_{k'\uparrow} \rangle \right) \tag{23}$$

$$\langle \gamma_{k'\uparrow}^\dagger \gamma_{k'\uparrow} \rangle = \langle \gamma_{-k'\downarrow}^\dagger \gamma_{-k'\downarrow} \rangle = \frac{1}{e^{\beta E_1 \ (k')} + 1} \tag{24}$$

Yielding

$$\langle \gamma_{-k'\downarrow} \gamma_{-k'\downarrow}^\dagger \rangle - \langle \gamma_{k'\uparrow}^\dagger \gamma_{k'\uparrow} \rangle = 1 - \frac{2}{e^{\beta E_1 (k')} + 1}$$

$$= \frac{e^{\beta E_1(k')} - 1}{e^{\beta E_1(k')} + 1}$$

$$= \tanh\left(\frac{E_1(k')}{2k_B T}\right) \quad (25)$$

From Eqs. (14) and (15), we also have:

$$u_{k'}^* v_{k'} = |u_k|^2 = \frac{1}{2}\left(1 + \frac{\xi_k}{\sqrt{\xi_k^2 + |\Delta_{SC}|^2}}\right)\left(\frac{\sqrt{\xi_k^2 + |\Delta_{SC}|^2} - \xi_k}{\Delta_{SC}^*}\right) = \frac{\Delta_{SC'}}{2\sqrt{\xi_{k'}^2 + |\Delta_{SC'}|^2}} \quad (26)$$

Yielding the gap equation:

$$\Delta_{SC} = -\sum_{k'} \frac{V_{kk'}^{SC} \Delta_{SC'}}{2E_1(k')} \tanh\left(\frac{E_1\ (k')}{2k_B T}\right) \quad (27)$$

By taking $V_{kk'}^{SC} = -V_0$ and $\Delta_{SC'} = \Delta_{SC}$, we obtain the BCS expression.

$$\frac{V_C}{K_\beta T_C} = 1.76$$

3.2.2. The Order Parameter of Spin Density Wave (SDW)

In this section we want to drive an expressions for the order parameters of SDW, Δ_{SDW}. Still we can use the Hamiltonian given by equation (1).

$$H_{SDW} = \sum_{KK'\sigma} V_{KK,'\sigma}^{SDW} C_{K,\sigma}^\dagger C_{K+q,\sigma} C_{k'+q,\bar{\sigma}}^\dagger C_{K',\bar{\sigma}} \quad (28)$$

With spin σ which is opposite to spin$\bar{\sigma}$, to decouple the Hamiltonian we use the mean field approximation. To proceed, we perform the usual mean-field decoupling of the quartic term.

$$\langle C_{K,\sigma}^\dagger C_{K+q,\sigma} C_{k'+q,\bar{\sigma}}^\dagger C_{K',\bar{\sigma}} \rangle = \langle C_{K,\sigma}^\dagger C_{K+q,\sigma} \rangle C_{k'+q,\bar{\sigma}}^\dagger C_{K',\bar{\sigma}} + C_{K,\sigma}^\dagger C_{K+q,\sigma} \langle C_{k'+q,\bar{\sigma}}^\dagger C_{K',\bar{\sigma}} \rangle - \langle C_{K,\sigma}^\dagger C_{K+q,\sigma} \rangle \langle C_{k'+q,\bar{\sigma}}^\dagger C_{K',\bar{\sigma}} \rangle \quad (29)$$

When we substitute equation (29) in to equation (28) it becomes:

$$H_{SDW} = \sum_{KK'\sigma} V_{KK,'\sigma}^{SDW} \langle C_{K,\sigma}^\dagger C_{K+q,\sigma} \rangle C_{k'+q,\bar{\sigma}}^\dagger C_{K',\bar{\sigma}} + C_{K,\sigma}^\dagger C_{K+q,\sigma} \langle C_{k'+q,\bar{\sigma}}^\dagger C_{K',\bar{\sigma}} \rangle - \langle C_{K,\sigma}^\dagger C_{K+q,\sigma} \rangle \langle C_{k'+q,\bar{\sigma}}^\dagger C_{K',\bar{\sigma}} \rangle \quad (30)$$

The mean field Hamiltonian of spin density wave can be expressed as:

$$H_{SDW} = -\sum_{k,\sigma}(\Delta_{SDW}\, C^{\dagger}_{k'+q,\bar{\sigma}} C_{K',\bar{\sigma}} + \Delta^{*}_{SDW} C^{\dagger}_{k'+q,\bar{\sigma}} C_{K',\bar{\sigma}}) + \sum_{k,\sigma} \Delta_{SDW} \langle C^{\dagger}_{k'+q,\bar{\sigma}} C_{K',\bar{\sigma}} \rangle \qquad (31)$$

Where the mean field is:

$$\Delta_{SDW} = -\sum_{k,\sigma} V^{SDW}_{KK,'\sigma} \langle C^{\dagger}_{K,\sigma} C_{K+q,\sigma} \rangle \qquad (32)$$

3.2.2.1. Bogoliubov Transformation in Spin Density Wave (SDW)

The annihilation and creation operators $C_{K,\sigma}$ and $C^{\dagger}_{K+q,\sigma}$ satisfy the anticommutation relation for fermions

$$C_{K,\sigma} = u_k \gamma^{\dagger}_{k,\sigma} + v_k \gamma^{\dagger}_{k+q,\sigma}$$

$$C^{\dagger}_{K+q,\sigma} = \sigma(v_k \gamma^{\dagger}_{k,\sigma} - u_k \gamma^{\dagger}_{k+q,\sigma}) \qquad (33)$$

The normalization condition of the complex coefficients u_k, v_k is:

$$|u_k|^2 + |v_k|^2 = 1 \qquad (34)$$

Then when we substitute in equation (31) it becomes:

$$-\sum_{k,\sigma}(\Delta_{SDW}\, C^{\dagger}_{k'+q,\bar{\sigma}} C_{K',\bar{\sigma}} + \Delta^{*}_{SDW} C^{\dagger}_{k'+q,\bar{\sigma}} C_{K',\bar{\sigma}})$$

$$= \sum_{k,\sigma}[(\Delta_k u_k v^{*}_k + \Delta^{*}_k u^{*}_k v_k)\,(\gamma^{\dagger}_{k,\sigma}\gamma_{k,\sigma} + \gamma^{\dagger}_{k+q,\sigma}\gamma_{k+q,\sigma}) - (\Delta_k u_k v^{*}_k + \Delta^{*}_k u^{*}_k v_k)]$$

$$-\sum_{k,\sigma}[\,(\Delta_k u_k^2 - \Delta^{*}_k v_k^2)\gamma^{\dagger}_{k,\sigma}\gamma^{\dagger}_{k+q,\sigma} + (\Delta^{*}_k (u^{*}_k)^2 - \Delta_k (u^{*}_k)^2)\gamma_{k+q,\sigma}\gamma^{\dagger}_{k,\sigma}] \qquad (35)$$

Therefore, the effective Hamiltonian is:

$$H_{SDW} = \sum_{k,\sigma}[(\Delta_k u_k v^{*}_k + \Delta^{*}_k u^{*}_k v_k)\,(\gamma^{\dagger}_{k,\sigma}\gamma_{k,\sigma} + \gamma^{\dagger}_{k+q,\sigma}\gamma_{k+q,\sigma}) - (\Delta_k u_k v^{*}_k + \Delta^{*}_k u^{*}_k v_k)]$$

$$-\sum_{k,\sigma}[\,(\Delta_k u_k^2 - \Delta^{*}_k v_k^2)\gamma^{\dagger}_{k,\sigma}\gamma^{\dagger}_{k+q,\sigma} + (\Delta^{*}_k (u^{*}_k)^2 - \Delta_k (u^{*}_k)^2)\gamma_{k+q,\sigma}\gamma^{\dagger}_{k,\sigma}]$$

$$+\sum_{k,\sigma} \Delta_{SDW} \langle C^{\dagger}_{k'+q,\bar{\sigma}} C_{K',\bar{\sigma}} \rangle \qquad (36)$$

For a three-dimensional s-wave superconductor with the quasiparticle excitation energy

$$E_2(k) = \sqrt{\left(\xi_{k+q}\right)^2 + \Delta_{k+q}^2} \tag{37}$$

Then we can write effective Hamiltonian as:

$$H_{SDW} = \sum_{k,\sigma} (\xi_k - E_2(k) + \Delta_{SDW} \langle C_{k'+q,\bar{\sigma}}^{\dagger} C_{K',\bar{\sigma}} \rangle) \tag{38}$$

Note that, a Bogoliubon is a mixture of electrons and holes:

$$\gamma_{k,\sigma} = u_k C_{K,\sigma} - v_k C_{K+q,\sigma}^{\dagger}$$

$$\gamma_{k+q,\sigma} = u_k^* C_{K+q,\sigma}^{\dagger} + v_k^* C_{K,\sigma} \tag{39}$$

3.2.2.2. The Gap Equation

We still need to determine the gap functionΔ_{SDW}, given self-consistently by Eq. (32).

$$\Delta_{SDW} = \sum_{KK',\sigma} V_{KK',\sigma}^{SDW} C_{K,\sigma}^{\dagger} C_{K+q,\sigma}^{\dagger} \tag{40}$$

Using the Bogoliubov transformation (33),$C_{K,\sigma} C_{K+q,\sigma}^{\dagger}$ becomes:

$$C_{K,\sigma} C_{K+q,\sigma}^{\dagger} = (u_k \gamma_{k,\sigma}^{\dagger} + v_k \gamma_{k+q,\sigma}^{\dagger}) \sigma (v_k \gamma_{k,\sigma}^{\dagger} - u_k \gamma_{k+q,\sigma}^{\dagger})$$

$$= u_k^* v_k (\gamma_{k,\sigma}^{\dagger} \gamma_{k,\sigma} - \gamma_{k+q,\sigma}^{\dagger} \gamma_{k+q,\sigma})$$

$$= u_k^* v_k \left[\tanh\left(\frac{E_2(k,\sigma)}{2K_B T}\right) - \tanh\left(\frac{E_2(k+q,\sigma)}{2K_B T}\right) \right] \tag{41}$$

From the coefficientsu_k,v_k we can get:

$$u_{k'}^* v_{k'} = |u_k|^2 = \frac{1}{2} \left(1 + \frac{\xi_k}{\sqrt{\left(\xi_{k+q}\right)^2 + \Delta_{k+q}^2}} \right) \left(\frac{\sqrt{\left(\xi_{k+q}\right)^2 + \Delta_{k+q}^2} - \xi_k}{\Delta_k^*} \right) = \frac{\Delta_{k'}}{2\sqrt{\left(\xi_{k+q}\right)^2 + \Delta_{k+q}^2}}$$

$$= \frac{\Delta_{k'}}{2E_2(k)} \tag{42}$$

Therefore, we obtain the self-consistency equation for the pair potential and gap equation becomes:

$$\Delta_{SDW}=\sum_{KK',\sigma} V^{SDW}_{KK,'\sigma}\frac{\Delta_{k'}}{2E_2(k)}\left[\tanh\left(\frac{E_2(k,\sigma)}{2K_BT_{sdw}}\right)-\tanh\left(\frac{E_2(k+q,\sigma)}{2K_BT_{sdw}}\right)\right] \quad (43)$$

3.2.3. The Order Parameter of Superconductivity and Spin Density Wave (SDW)

The Hamiltonian in the coexistence state is in the following. We separate it into three terms

$$H = H_1 + H_2 + H_3 \quad (44)$$

$$H_1 = \sum_{k,\delta} \xi_k\, C^\dagger_{k\delta} C_{k\delta}$$

$$H_2 = \sum_{kk'} V^S_{kk'}\, C^\dagger_{k\uparrow} C^\dagger_{-k\downarrow} C_{-k'\downarrow} C_{k'\uparrow}$$

$$H_3 = \sum_{KK'\sigma} V^{SDW}_{KK,'\sigma} C^\dagger_{K,\sigma} C_{K+q,\sigma} C^\dagger_{k'+q,\bar{\sigma}} C_{K',\bar{\sigma}}$$

From equation (2) we have:

$$\hat{H}_{SC} = H_1 + H_2 \quad and$$

$$\hat{H}_{SDW} = \hat{H}_3$$

So

$$H = H_{SC} + H_{SDW} \quad (45)$$

However

$$H_{SC} = \sum_{k,\delta} \xi_k\, C^\dagger_{k\delta} C_{k\delta} + \sum_{kk'} V^S_{kk'}\, C^\dagger_{k\uparrow} C^\dagger_{-k\downarrow} C_{-k'\downarrow} C_{k'\uparrow}$$

Then

$$H = \sum_{k,\delta} \xi_k\, C^\dagger_{k\delta} C_{k\delta} + \sum_{kk'} V^S_{kk'}\, C^\dagger_{k\uparrow} C^\dagger_{-k\downarrow} C_{-k'\downarrow} C_{k'\uparrow} + \sum_{KK'\sigma} V^{SDW}_{KK,'\sigma} C^\dagger_{K,\sigma} C_{K+q,\sigma} C^\dagger_{k'+q,\bar{\sigma}} C_{K',\bar{\sigma}} \quad (46)$$

Using the above equation (6) & (30) into equation (45)

The effective Hamiltonian becomes:

$$\hat{H} = \sum_{k,\delta} \xi_k C^{\dagger}_{k\delta} C_{k\delta} - \sum_{k} \left(\Delta_{SC} C^{\dagger}_{k\uparrow} C^{\dagger}_{-k\downarrow} + \Delta^{*}_{k} C_{-k\downarrow} C_{k\uparrow} \right) + \sum_{k} \Delta_k \langle C^{\dagger}_{k\uparrow} C^{\dagger}_{-k\downarrow} \rangle$$
$$- \sum_{k,\sigma} (\Delta_{SDW}\, C^{\dagger}_{k'+q,\bar{\sigma}} C_{K',\bar{\sigma}} + \Delta^{*}_{SDW} C^{\dagger}_{k'+q,\bar{\sigma}} C_{K',\bar{\sigma}}) + \sum_{k,\sigma} \Delta_{SDW} \langle C^{\dagger}_{k'+q,\bar{\sigma}} C_{K',\bar{\sigma}} \rangle \quad (47)$$

Where the mean field is:

$$\Delta_{SDW} = -\Delta_{SC} \sum_{kk'} V^{SC}_{kk'}\, V^{SDW}_{KK,'\sigma} \langle C_{-k'\downarrow} C_{k'\uparrow} \rangle + \langle C^{\dagger}_{K,\sigma} C_{K+q,\sigma} \rangle \quad (48)$$

3.2.3.1. Bogoliubov Transformation in Superconductivity and Spin Density Wave (SDW)

To solve the above equation, we use Bogoliubov Transformation.

$$C_{k\uparrow} = u^{*}_{k} \gamma_{k\uparrow} + v_k \gamma^{\dagger}_{-k\downarrow}$$

$$C^{\dagger}_{-k\downarrow} = u_k \gamma^{\dagger}_{-k\downarrow} - v^{*}_{k} \gamma_{k\uparrow}$$

$$C_{K,\sigma} = u_k \gamma^{\dagger}_{k,\sigma} + v_k \gamma^{\dagger}_{k+q,\sigma}$$

$$C^{\dagger}_{K+q,\sigma} = \sigma (v_k \gamma^{\dagger}_{k,\sigma} - u_k \gamma^{\dagger}_{k+q,\sigma}) \quad (49)$$

The normalization condition of the complex coefficients u_k, v_k is:

$$|u_k|^2 + |v_k|^2 = 1$$

Then substituting in equation (47), the effective Hamiltonian becomes:

$$\hat{H} = \sum_{k} [2\xi_k |v_k|^2 - \Delta_{SC} u_k v^{*}_{k} - \Delta^{*}_{SC} u^{*}_{k} v_k + \Delta_{SC} \langle C^{\dagger}_{k\uparrow} C^{\dagger}_{-k\downarrow} \rangle]$$
$$+ \sum_{k} [\xi_k (|u_k|^2 - |v_k|^2) + \Delta_{SC} u_k v^{*}_{k} + \Delta^{*}_{SC} u^{*}_{k} v_k] (\gamma^{\dagger}_{k\uparrow} \gamma_{k\uparrow} + \gamma^{\dagger}_{-k\downarrow} \gamma_{-k\downarrow})$$
$$+ \sum_{k} [2\xi_k u_k v_k - \Delta_k u^2_k + \Delta^{*}_{SC} v^2_k] (\gamma^{\dagger}_{k\uparrow} \gamma^{\dagger}_{-k\downarrow}) + \sum_{k,\sigma} [(\Delta_k u_k v^{*}_{k} + \Delta^{*}_{k} u^{*}_{k} v_k)\, (\gamma^{\dagger}_{k,\sigma} \gamma_{k,\sigma}$$
$$+ \gamma^{\dagger}_{k+q,\sigma} \gamma_{k+q,\sigma}) - (\Delta_k u_k v^{*}_{k} + \Delta^{*}_{k} u^{*}_{k} v_k)]$$
$$- \sum_{k,\sigma} [\, (\Delta_k u^2_k - \Delta^{*}_{k} v^2_k) \gamma^{\dagger}_{k,\sigma} \gamma^{\dagger}_{k+q,\sigma} + (\Delta^{*}_{k} (u^{*}_{k})^2 - \Delta_k (u^{*}_{k})^2) \gamma_{k+q,\sigma} \gamma^{\dagger}_{k,\sigma}]$$
$$+ \sum_{k,\sigma} \Delta_{SDW} \langle C^{\dagger}_{k'+q,\bar{\sigma}} C_{K',\bar{\sigma}} \rangle + h.c \quad (50)$$

Using equation (17) and (37), it becomes

$$\hat{\mathrm{H}} = \sum_{k\sigma} E_1(k)\gamma_{k\sigma}^{\dagger}\gamma_{k\sigma} + \sum_{k}\left(\xi_k - E_k + \Delta_k\langle \mathrm{C}_{k\uparrow}^{\dagger}\mathrm{C}_{-k\downarrow}^{\dagger}\rangle\right)$$
$$+ \sum_{k,\sigma}(\xi_k - E_2(k) + \Delta_{SDW}\,\langle C_{k'+q,\bar{\sigma}}^{\dagger} C_{K',\bar{\sigma}}\rangle) \quad (51)$$

$$\hat{\mathrm{H}} = \sum_{k\sigma} E_1(k)\gamma_{k\sigma}^{\dagger}\gamma_{k\sigma} + E_0 + \sum_{k,\sigma}(\xi_k - E_2(k) + \Delta_{SDW}\,\langle C_{k'+q,\bar{\sigma}}^{\dagger} C_{K',\bar{\sigma}}\rangle) \quad (52)$$

Where

$$E_0 = \sum_{k}\left(\xi_k - E_k + \Delta_k\langle \mathrm{C}_{k\uparrow}^{\dagger}\mathrm{C}_{-k\downarrow}^{\dagger}\rangle\right)$$

Note that, a Bogoliubon is a mixture of electrons and holes:

$$\gamma_{k\uparrow} = u_k \mathrm{C}_{k\uparrow} - v_k \mathrm{C}_{-k\downarrow}^{\dagger}$$

$$\gamma_{-k\downarrow} = u_k^{*}\mathrm{C}_{-k\downarrow}^{\dagger} + v_k^{*}\mathrm{C}_{k\uparrow}$$

$$\gamma_{k,\sigma} = u_k C_{K,\sigma} - v_k C_{K+q,\sigma}^{\dagger}$$

$$\gamma_{k+q,\sigma} = u_k^{*} C_{K+q,\sigma}^{\dagger} + v_k^{*} C_{K,\sigma} \quad (53)$$

3.2.3.2. The Gap Equation

We will need to determine the gap functionΔ_{SDW}, given by:

$$\Delta_{SDW} = -\Delta_{SC}\sum_{kk'} V_{kk'}^{SC}\, V_{KK,'\sigma}^{SDW}\langle \mathrm{C}_{-k'\downarrow}\mathrm{C}_{k'\uparrow}\rangle + \langle C_{K,\sigma}^{\dagger} C_{K+q,\sigma}\rangle \quad (54)$$

By evaluating both the SDW coherence factors and the BCS coherence factors, we get the final self-consistent equation for Δ_{SDW} and Δ_{SC} in the coexistence state as

$$\Delta_{SDW} = \Delta_{SC}\sum_{k\in R}\frac{\Delta_{SDW}}{2E(k)}\left[\frac{E_k^{\alpha}}{\Omega_k^{\alpha}}\tanh\left(\frac{\Omega^{\alpha}}{2K_B T_C}\right) - \frac{E_k^{\alpha}}{\Omega_k^{\alpha}}\tanh\left(\frac{\Omega^{\beta}}{2K_B T_C}\right)\right] \quad (55)$$

CHAPTER 4

4. RESULT AND DISCUSSION

In this section, we describe the results which are obtained by developing a model Hamiltonian for the system and using diagonalized Bogoliubov transformation, and obtain the expressions for the superconducting order parameter (Δ_{SC}) and magnetic order parameter (Δ_{SDW}) with respect to superconducting transition temperature (Tc) and magnetic transition temperature (T_{SDW}) respectively. First, using Equation (27) and the experimental value of Tc for the superconducting ($Ba\ (Fe_{1-x}Co_x)_2\ As_2$) we plotted the transition temperature (Tc) versus superconducting order parameter (Δ_{SC}) as shown in Figure 4.1. As can be seen from the figure, when the superconducting order parameter increases the superconducting transition temperature decreases and vanishes as the temperature is equal to the critical temperature. Second, by employing Equation (43) and the experimental value, $T_{SDW} \approx 0.67$ K for ($Ba\ (Fe_{1-x}Co_x)_2\ As_2$) and some suitable approximations for the other parameters in the equation, we plotted the magnetic transition temperature (T_{SDW}) versus magnetic order parameter (Δ_{SDW}) as demonstrated in Figure 4.2. From the figure, it is vivid that, as the magnetic order parameter (Δ_{SDW}) increases the magnetic transition temperature (T_{SDW}) also increases. Using equations (55) and by considering some plausible approximations, we plotted the phase diagrams of superconducting transition temperature (T_C) versus magnetic order parameter (Δ_{SDW}), in the commensurate magnetism and superconductivity in electron-doped barium iron arsenide superconductor, as shown in Figure 4.3.Which shows that as the magnetic order parameter (Δ_{SDW})increases the superconducting transition temperature (Tc) decreases and vanishes as the temperature is equal to the critical temperature. The green line is the first-order transition line between commensurate and incommensurate SDW phases. By merging Figs. 4.2 and 4.3, we have demonstrated the region where both superconductivity and ferromagnetism can coexists in Fig. 4.4.Clearly the figure demonstrates the strong competition between the SC and SDW phases emphasizing the coexistence of SDW and superconductivity at low magnetic order parameter. The coexistence phase between SC and (in)commensurate SDW orders does exist at lower superconducting transition temperature (Tc). The commensurate SDW order appears below the structural transition temperature and SC coexists with SDW order in under doped region. Near optimal superconductivity, it has been shown that the commensurate SDW order changes into transversely incommensurate SDW order that coexists and competes with superconductivity.

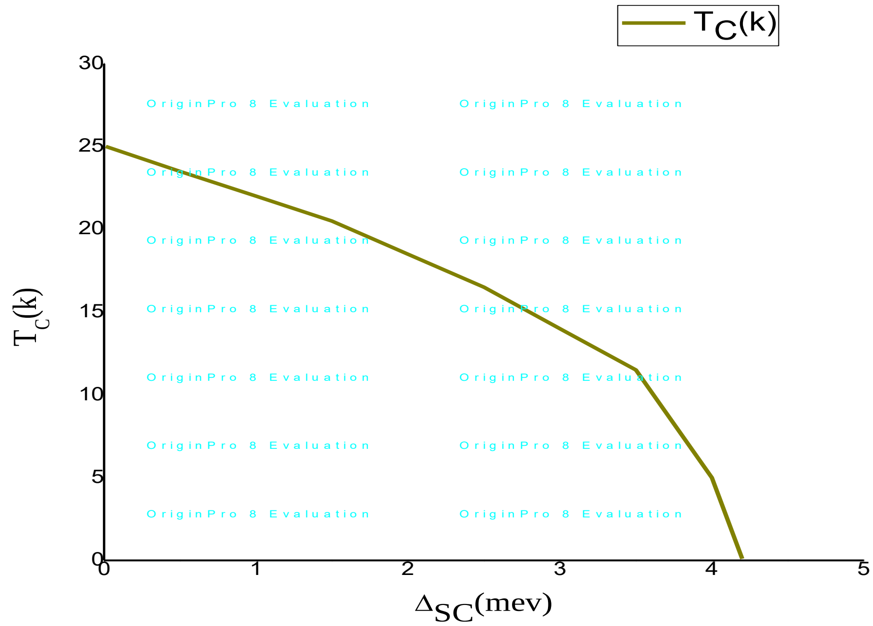

Figure 4.1Phase diagram of superconducting order parameter (Δ_{SC}) vs. superconducting transition temperature (Tc)for (Ba $(Fe_{1-x}Co_x)_2As_2$)superconductor

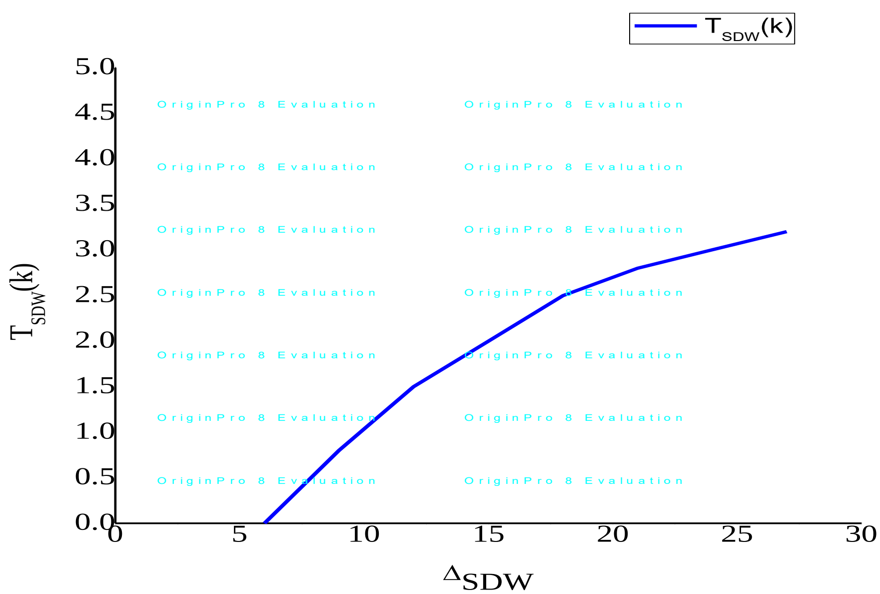

Figure 4.2 Phase diagram of magnetic order parameter (Δ_{SDW}) vs. magnetic transition temperature (T_{SDW})for (Ba $(Fe_{1-x}Co_x)_2As_2$)superconductor.

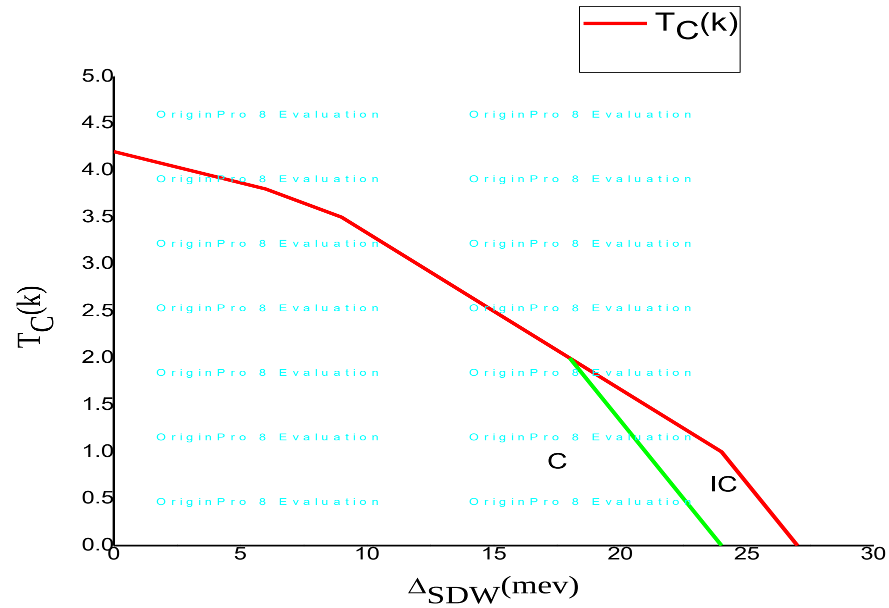

Figure 4.3 Phase diagram of magnetic order parameter (Δ_{SDW}) vs. superconducting transition temperature (Tc) and the transition between commensurate and incommensurate SDW phases for (Ba $(Fe_{1-x}Co_x)_2 As_2$) superconductor.

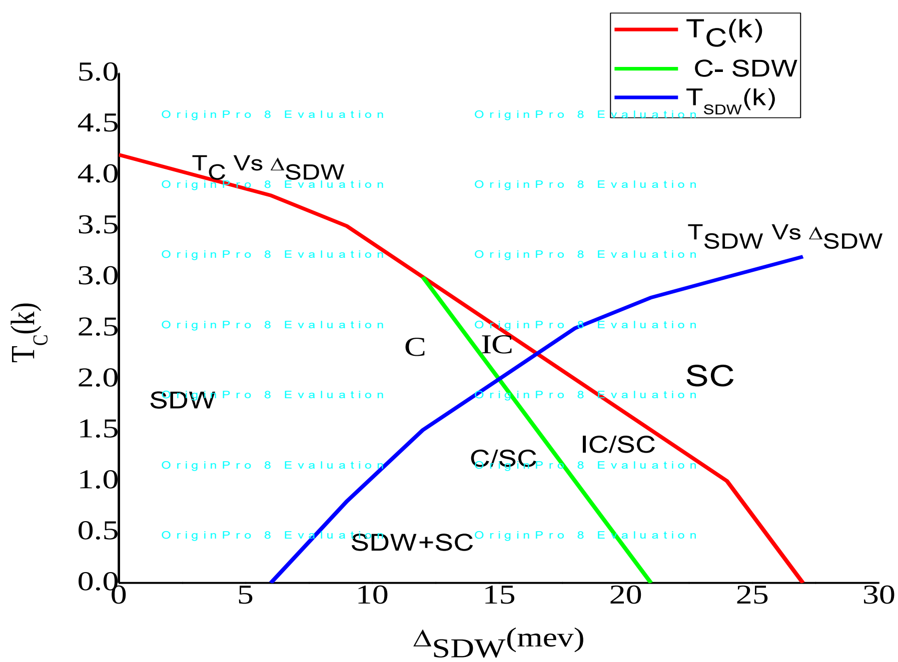

Figure 4.4 Phase diagram of superconducting transition temperature (Tc), magnetic transition temperature (T_{SDW}), versus magnetic order parameter (Δ_{SDW}). The figure demonstrates the coexistence phase between SC and (in) commensurate SDW orders.

From the above figures, no incommensurate (IC) magnetic ordering exists in < 5.4% Co substituted $BaFe_2As_2$ compounds. The commensurate(C)-to-incommensurate(IC) transition is seen in > 5.4% Co substitution. The commensurate SDW order appears below the structural transition temperature and SC coexists with SDW order in under doped region. The commensurate SDW order changes into transversely incommensurate SDW order that coexists and competes with superconductivity.

CHAPTER 5

5. CONCLUSION

In this thesis we have analyzed theoretically the coexistence of C/IC-SDW and superconductivity in ($Ba(Fe_{1-x}Co_x)_2As_2$). In the first two chapters, we have presented a brief introduction and a review of previous works which had been carried out by other researchers that are pertinent to our work. In chapter three and four we discussed the interplay of C/IC-SDW and superconductivity in ($Ba(Fe_{1-x}Co_x)_2As_2$) where we derived expressions by developing a model Hamiltonian for the system and using diagonalized Bogoliubov transformation which demonstrate the relation between the order parameters of these states and we plot graphs which show the behavior of these order parameters with increasing temperature. When the superconducting order parameter increases the superconducting transition temperature decreases. From figure (4.4) when the magnetic order parameter (Δ_{SDW}) increases, the superconducting transition temperature decreases, the magnetic transition temperature (T_{SDW}) increases. The commensurate SDW order appears below the structural transition temperature and SC coexists with SDW order in under doped region. Electron doped 122 FebSCs confirmed that commensurate long range AFM coexist with SC in under doped region. In addition, for electron doped Ba122 samples near optimal SC, it has been shown that the commensurate static AFM order changes into transversely incommensurate short range AFM order that coexists and competes with superconductivity.

BIBLIOGRAPHY

[1] Onnes, H.K. (1911) the Superconductivity of Mercury. Comm. Phys. Lab. Univ., Leiden, 122-124.

[2] Girma Kitachew Jenberie, superconductivity and anti-ferromagnetic spin density wave in iron based superconductors, 1, January, 2015.

[3] Zhao-Sheng Wang, The superconducting properties research of iron based-122 by transport and scanning micro-squid measurements, 2, Mar 2015

[4] W. Meissner and R. Ochsenfeld. Ein neuer Effekt bei Eintritt der Supraleitfaehigkeit. Naturwissenschaften, 21:787, 1933.

[5] Zhao-Sheng Wang, The superconducting properties research of iron based-122 by transport and scanning micro-squid measurements, 3, Mar 2015

[6] J. Bardeen, L. N. Cooper, and J.R. Schrieffer. Microscopic theory of superconductivity. Phys. Rev., 106:162–164, 1957.

[7] J.Bardeen, L. N. Cooper, and J.R. Schrieffer. Theory of superconductivity. Phys. Rev., 108:1175, 1957.

[8] Bednorz, J. George, and K. Alex Muller, Ten Years of Superconductivity: 1980-1990, Springer Netherlands, 1986. 267 - 271.

[9] Y. Kamihara, H. Hiramatsu, M. Hirano, R. Kawamura, H. Yanagi, T. Kamiya, and H. Hosono, Iron-based layered superconductor: LaOFeP,J. Am. Chem. Soc. 128, 10012 (2006).

[10] Y. Kamihara, T. Watanabe, M. Hirano, and H. Hosono, Iron-Based Layered Superconductor La (O1-xFx)FeAs (x = 0.05-0.12) with Tc = 26 K, J. Am. Chem. Soc. 130, 3296 (2008).

[11] H. Takahashi, K. Igawa, K. Arii, Y. Kamihara, M. Hirano, and H. Hosono, Superconductivity at 43 K in an iron-based layered com pound LaO1-xFxFeAs, Nature 453, 376 (2008).

37

[12] Zhao-Sheng Wang, The superconducting properties research of iron based-122 by transport

and scanning micro-squid measurements,10, Mar 2015
[13] J. Wen, G. Xu, G. Gu, J. M. Tranquada, and R. J. Birgeneau. Interplay between magnetism and superconductivity in iron-chalcogenide superconductors: crystal growth and characterizations. Reports on Progress in Physics, 74(12):124503, December 2011.
[14] Johnpierre Paglione and Richard L. Greene. High-temperature superconductivity in ironbased materials. Nature Physics, 6(9):645–658, September 2010.
[15] Y. Kamihara, T. Watanabe, M. Hirano, and H. Hosono, Iron-Based Layered Superconductor La(O1-xFx)FeAs (x = 0.05-0.12) with Tc = 26 K, J. Am. Chem. Soc. 130, 3296 (2008).
[16] Johnpierre Paglione and Richard L. Greene. High-temperature superconductivity in ironbased materials. Nature Physics, 6(9):645–658, September 2010.
[17] A. Leithe-Jasper, W. Schnelle, C. Geibel, H. Rosner, '122' Family Bases Superconductors Phys. Rev. Lett. 101 (2008) 207004.
[18] A.S. Sefat, R. Jin, M.A. McGuire, B.C. Sales, D.J. Singh, D. Mandrus, '122' Family Bases Superconductors, Phys. Rev. Lett. 101 (2008) 117004.
[19] N. Ni, M.E. Tillman, J.-Q. Yan, A. Kracher, S.T. Hannahs, S.L. Bud'ko, P.C. Canfield, '122' Family Bases Superconductors, Phys. Rev. B 78 (2008) 214515.
[20] S. Sharma, A. Bharathi, S. Chandra, R. Reddy, S. Paulraj, A. Satya, V. Sastry, A. Gupta, C. Sundar, '122' Family Bases Superconductors, Phys. Rev. B 81 (2010) 174512.
[21] W. Schnelle, A. Leithe-Jasper, R. Gumeniuk, U. Burkhardt, D. Kasinathan, H. Rosner, '122' Family Bases Superconductors ,Phys. Rev. B 79 (2009) 214516.
[22] M. Rotter, M. Tegel, D. Johrendt, '122' Family Bases Superconductors, Phys. Rev. Lett. 101 (2008) 107006.
[23] Zhi Ren, Qian Tao, Shuai Jiang, Chunmu Feng, Cao Wang, Jianhui Dai, Guanghan
38
Cao, Zhu'an Xu, '122' Family Bases Superconductors Phys. Rev. Lett. 102 (2009) 137002.
[24] Shuai Jiang, Hui Xing, Guofang Xuan, Cao Wang, Zhi Ren, Chunmu Feng, Jianhui

Dai, Zhu'an Xu, Guanghan Cao, J'122' Family Bases Superconductors, Phys. Condens. Matter 21 (2009) 382203.

[25] S. Kasahara, T. Shibauchi, K. Hashimoto, K. Ikada, S. Tonegawa, R. Okazaki, H. Shishido, H. Ikeda, H. Takeya, K. Hirata, T. Terashima, Y. Matsuda, '122' Family Bases Superconductors, Phys. Rev. B 81 (2010) 184519.

[26] S.R. Saha, N.P. Butch, K. Kirshenbaum, Johnpierre Paglione, P.Y. Zavali, '122' Family Bases Superconductors, Phys. Rev. Lett. 103 (2009) 037005.

[27] A. Martinelli, F. Bernardini, S. Massida, The phase diagrams of iron-based superconductors: theory and experiments, C. R. Physique 17 (1–2) (2016) 5–35, this issue.

[28] Krzysztof Gofryk, Minghu Pan, Claudia Cantoni, Bayrammurad Saparov, Jonathan E. Mitchell, Athena S. Sefat, Phys. Rev. Lett. 112 (2014) 047005.

[29] F. Krüger, S. Kumar, J. Zaanen, J. van den Brink, Spin-orbital frustrations and anomalous metallic state in iron-pnictide superconductors, Phys. Rev. B 79 (2009) 054504

[30] W. Lv, J. Wu, P. Phillips, Orbital ordering induces structural phase transition and the resistivity anomaly in iron pnictides, Phys. Rev. B 80 (2009) 224506

[31] C.-C. Chen, J. Maciejko, A. P. Sorini, B. Moritz, R. R. P. Singh, T. P. Devereaux, Orbital order and spontaneous orthorhombicity in iron pnictides, Phys. Rev. B 82 (2010) 100504(R)

[32] R. M. Fernandes, A. V. Chubukov, J. Knolle, I. Eremin, J. Schmalian, Preemptive nematic order, pseudogap, and orbital order in the iron pnictides, Phys. Rev. B 85 (2012) 024534; Erratum Phys. Rev. B 85 (2012) 109901

[33] J. Dong, H. J. Zhang, G. Xu, Z. Li, G. Li, W. Z. Hu, D. Wu, G. F. Chen, X. Dai, J. L. Luo, Z. Fang, N. L. Wang, Competing orders and spin-density-wave instability in LaO1-xFxFeAs Europhys. Lett. 83 (2008) 27006

39

[34] C. Marini, C. Mirri, G. Profeta, S. Lupi, D. Di Castro, R. Sopracase, P. Postorino, P. Calvani, A. Perucchi, S. Massidda, G. M. Tropeano, M. Putti, A. Martinelli, A. Palenzona, P. Dore, The optical phonon spectrum of SmFeAsO, EPL 84 (2008) 67013

[35] V. Brouet, M. Marsi, B. Mansart, A. Nicolaou, A. Taleb-Ibrahimi, P. Le Fèvre, F. Bertran, F. Rullier-Albenque, A. Forget, D. Colson, Phys. Rev. B 80 (2009) 165115.

[36] S. Ideta, T. Yoshida, I. Nishi, A. Fujimori, Y. Kotani, K. Ono, Y. Nakashima, S. Yamaichi, T. Sasagawa, M. Nakajima, K. Kihou, Y. Tomioka, C.H. Lee, A. Iyo, H. Eisaki, T. Ito, S. Uchida, R. Arita, Phys. Rev. Lett. 110 (2013) 107007.

[37] H. Wadati, I. Elfimov, G.A. Sawatzky, Phys. Rev. Lett. 105 (2010) 157004.

[38] P.C. Canfield, S.L. Bud'ko, Annu. Rev. Condens. Matter Phys. 1 (2010) 27–50.

[39] Bulgarian,J.physics. The new iron-base superconducting materials 40(2013)247-252

[40] G.R.Stewart, Rev.Mod.Phys.1589(2011)

[41] Rajikant, Applied solid state physics, Radbat offset, Delhi,511,(2011).

[42] Fan Yang, et al., The electronic instabilities of the iron-based superconductor: a variation Monte-Carlos study, arxiv: 1007.2643 v4[cond-mat. Strel](2011).

[43] Yang Shuo, et al., Competition of magnetism and superconductivity in FeAs-based materials 18,1674-1056(2009).

[44] Ma Long and Yu Wei-Qiang, Review of nuclear magnetic resonance studies on iron-,Chin.phys.B,22,087414(2013).

[45] Ewings, R.A.,Perring, T.G., Bewley, R.I., Guidi, T., Pitcher, M.J., Parker, D.R., Clarke, S.J., and Boothroyed, A. T. Dec 2008 phys. Rev. B 78,220501.

[46] Tegel, M., Weiß, V., Schappacher, F.M., Ṗottgen, R., and Johrendt, D. (2008) Journal of physics: Condensed Matter 20(45),452201.

[47] D.Schmidta H.F.Brauna, "Effect of antimony substitution in ironpnictide

40

compoundes",arxi:1510.08665v1[cond-mat.super-con] (2015).

[48] K.N.Upadhyaya, a text of inorganic chemistry, Vikas publishing house pvt ltd,

[49] M.Neupane, et al., " electron-hole Asymmetry in superconductivity of pnictides originated from the observed rigid chemical potential shift" arxiv:1005.2966v1[cond mat.super-con] (2003)

[50] Amil Kamar D.a text of organic chemistry, New age International Limited 466,(2003).

[51] Iron-based high transition temperature superconductors Xianhui chen 1, Pengcheng Dia2,3 Donglai Feng4, Tao Xiang3,5 and Fu-Chun Zhang6,* National science Review1:371-395,2014.

[52] superconductivity induced by Ni doping in BaFe2As2 single crystals, Department of physics, Zhejiang University, Hangzhuou 310027, peoples Republic of China, orxivi 0809,2009v2[cond.mat.supr.con](2008).

[53] Gitte Stieper, competing superconducting and magnetic order parameter and field induced magnetism in Ba(Fe0.95Co0.05)2As2 copenhagen University 9,2012.

[54] Dagne Atnafu Shiferaw, the study of coexistence of superconductivity and spin density wave (sdw) in SmO1-xFxFeAs,11, July 2010.

[55] S.Maiti,et al., Gap nodes induced by coexistence with anti-ferromagnetism in iron based superconductors, arxiv:1203.0991v1 [cond-mat.supr-con] (2012)

[56] N.Fujiwara, et al., detection of antiferromagnetic order in heavily doped LaFeAsO1- xHx pnictide superconductors using nuclear-magnetic-resonance techniques, arXiv:

1308.2125v1[cond-mat.supr-con] 6 Aug (2013).

[57] P.Bonville, et al. Incommensurate spin density wave in Co-doped BaFe2As2, EPL,89,67008(2010).

[58] J. H. Chu, J. G. Analytis, C. Kucharczyk, and I. R. Fisher, Determination of the Phase Diagram of the Electron-Doped Superconductor Ba(Fe1-xCox)2As2, Phys. Rev. B 79,

41

014506 (2009).

[59] X. F. Wang, T. Wu, G. Wu, R. H. Liu, H. Chen, Y. L. Xie, and X. H. Chen, The Peculiar Physical Properties and Phase Diagram of Ba(Fe1-xCox)2As2Single CrystalsW, New J. Phys. 11, 045003 (2009).

[60] N. Doiron-Leyraud, P. Auban-Senzier, S. Ren´e de Cotret, C. Bourbonnais, D. J´erome, K. Bechgaard, and L. Taillefer, Correlation between linear resistivity and Tc in the Bechgaard salts and the pnictide superconductor Ba(Fe1-xCox)2As2, Phys. Rev. B 80, 214531 (2009).

[61] F. L. Ning, K. Ahilan, T. Imai, A. S. Sefat, R. Y. Jin, M. A. McGuire, B. C. Sales, and

D. Mandrus, Spin Susceptibility, Phase Diagram, and Quantum Criticality in the Eelctron Doped High Tc Superconductor Ba(Fe1-xCox)2As2, J. Phys. Soc. Japan 78, 013711 (2009).

[62] Rein Huisman Phase diagram of Ba(Fe1-xCox)2As2pnictides using transport

measurement van der Waals-Zeeman Institute Faculty of science, university of

Amsteram,2010

[63] N. Fujiwara, et al., Detection of antiferromagnetic ordering in heavily doped

LaFeAsO1-xHx pnictide superconductors using nuclear-magnetic-resonance techniques,

arXive: 1308. 2125v1[cond-mat. Supr-con] 6 Aug (2013).

[64] M. Rotter, M. Tegel, D. Johrendt, I. Schellenberg, W. Hermes, and R. P¨ottgen, Spin density-wave anomaly at 140 K in the ternary iron arsenide Ba(Fe1-xCox)2As2, Phys. Rev. B

78, 020503 (2008).

[65] Girma Kitachew Jenberie, superconductivity and anti-ferromagnetic spin density wave in

iron based superconductors, 53, January, 2015.

[66] C.Lester,et al., Neutron scattering study of the interplay between structure and

magnetism in Ba(Fe1-xCox)2As2 physical review letters B 79 144523 (2009).